Joint Norwegian – Soviet Electron Diffraction Studies of Molecular Structures in the Gas Phase. II. Inorganic Compounds

Anatoli A. Ischenko,[a] Victor P. Spiridonov[a,*] and Tor G. Strand[b]

[a]Department of Chemistry, Moscow State University, Moscow 119899, U.S.S.R. and [b]Department of Chemistry, University of Oslo, P.O. Box 1033, Blindern, N-0315 Oslo 3, Norway

Ischenko, A. A., Spiridonov, V. P. and Strand, T. G., 1988. Joint Norwegian – Soviet Electron Diffraction Studies of Molecular Structures in the Gas Phase. II. Inorganic Compounds. – Acta Chem. Scand., Ser. A 42: 651–673.

Our results of gas-phase electron diffraction investigations on some Group V pentahalides are reviewed. The compounds in question are the pentachlorides of antimony, niobium and tantalum, as well as tantalum pentabromide. The free molecules all have trigonal bipyramidal structures of D_{3h} symmetry with axial bonds longer than the equatorial ones, and they pseudorotate against relatively low barriers. The possible mechanism of pseudorotation is discussed and the values obtained for the barriers by electron diffraction are compared to the values obtained by other methods.

The structures obtained by gas-phase electron diffraction of the oligomeric pentafluorides of niobium, tantalum, antimony and gold are compared and discussed.

Dedicated to Professor Otto Bastiansen on his 70th birthday

A. The structure and intramolecular motion of Group V pentahalides

Background

The structural chemistry of the pentahalides of group V elements is of considerable interest. The study of intramolecular rearrangements in these compounds is fruitful from the point of view of gaining insight into the kinetics and mechanisms of chemical reactions which are supposed to involve five-coordinate transient species.[1-9] The intramolecular exchange of atoms is known as polyhedral[10] or polytopic[11-13] rearrangement. Various molecular geometries corresponding to topologically related potential energy surface (PES) minima may be called topological isomers.[14] In trigonal-bipyramidal molecules containing five chemically identical ligands, ML_5, intramolecular exchange of the ligands is often referred to as pseudorotation,[15] since this exchange is equivalent to rotation of the molecule as a whole (Fig. 1). Sometimes this term is also applied to molecules with nonequivalent substituents.

All the Group V element pentahalides studied to date have trigonal-bipyramidal configurations of D_{3h} symmetry with the M–L_{ax} bonds elongated relative to the M–L_{eq} bonds, in agreement with VSEPR theory predictions.[16-20] Numerous X-ray studies of five-coordinate compounds in the solid state[20] have shown that another possible configuration of ML_5-type molecules is a square-pyramidal one of C_{4v} symmetry. Berry[15] was the first to suggest the transition $D_{3h} \leftrightarrow C_{4v} \leftrightarrow D'_{3h}$ (Fig. 1) whose net result was exchange of equatorial and axial ligands. Berry[15] also suggested that the pseudorotation mechanism involved quantum-mechanical tunneling between minima of a one-dimensional "two-well" potential function.

Berry's hypothesis[15] was advanced to explain the inconsistency of data on five-coordinate compounds obtained using various techniques. Thus, in isotopic exchange experiments[21,22] three of the five chlorine atoms in PCl_5 underwent exchange

* To whom correspondence should be addressed.

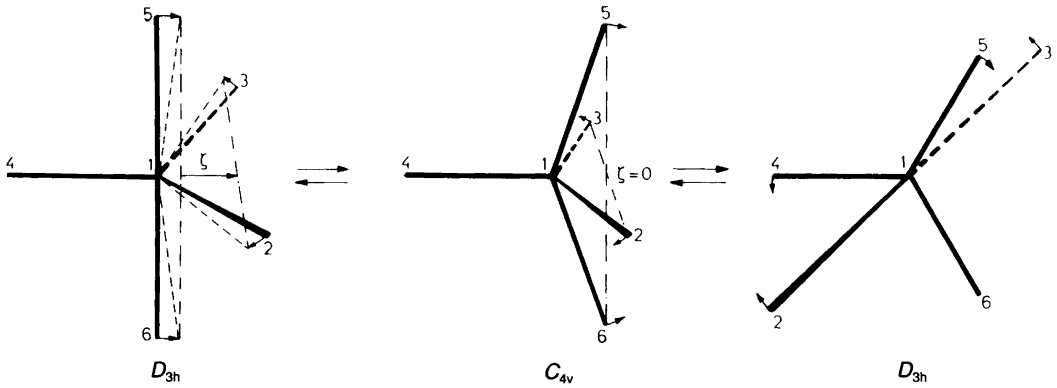

Fig. 1. Pseudorotation model for trigonal-bipyramidal ML_5 molecules.

far faster ($t_{1/2} \sim 5$ s) than the other two, for which only 90 % equilibration was attained in 100 min. NMR spectra of both gaseous and liquid phosphorus pentafluoride were, however, indicative of equivalence of all the fluorine atoms.[23–27] Such apparent equivalence can only be observed if the exchange is fast on the NMR time scale.[23–27] The investigations[23–26] were completed when the results of the electron diffraction studies on phosphorus pentafluoride[28] and pentachloride[29] were known. According to these investigations the molecules had trigonal-bipyramidal structures with non-equivalent halogen atoms in the equatorial and axial positions. In more recent studies on PF_5[30,31] and PCl_5[32] these structural conclusions were verified and the geometrical parameters of PF_5 and PCl_5 were determined with significantly higher accuracy. As has been shown using dynamic NMR techniques (Refs. 33–37), phosphoranes of the general formula PF_nL_{5-n} ($n = 1$–5) are also characterized by stereochemical non-rigidity (this term was first introduced in Refs. 10, 11 and 23; see also Refs. 33–50). At the same time, unambigous evidence was obtained from electron diffraction, and numerous X-ray and spectroscopic studies of these compounds for the presence of two types of chemical bonds in five-coordinate molecules, i.e. axial and equatorial (D_{3h}) or apical and basal (C_{4v}) bonds.

An explanation of the apparent differences in the molecular structures of five-coordinated compounds obtained in various experiments can be given if one recognizes the close relationship of the results to the different mean values obtained by the various physical techniques applied in studying free molecules and condensed matter.[38–50]

The pseudorotation model for pentahalides

A subject of continuing speculation is the pseudorotation model for pentahalides. One of the possible polytopic rearrangement paths in these compounds between two "nearest" topological isomers can be described by a two-minima potential function[51]

$$V(\xi) = V_0[(\xi/\xi_0)^2 - 1]^2 \qquad (1)$$

where the definition of the coordinate ξ follows from Fig. 1, and V_0 and ξ_0 are the barrier to pseudorotation and the potential curve saddle point position, respectively.

The potential function (1) is similar to that describing inversion vibrations in pyramidal molecules[52–61] such as ammonia.[52,55] Molecular symmetry and over-barrier transitions between the PES minima can then most accurately be described in terms of inversion-permutation symmetry groups (see, e.g., Refs. 8 and 9). Thus, if all the atoms are identical in an ML_5 molecule of symmetry D_{3h}, the number of possible topological isomers[14] can be shown to be:[54]

$$P = \frac{(5!)\times 2}{12} = 20$$

A molecule can therefore be delocalized between 20 PES minima and its description in terms of

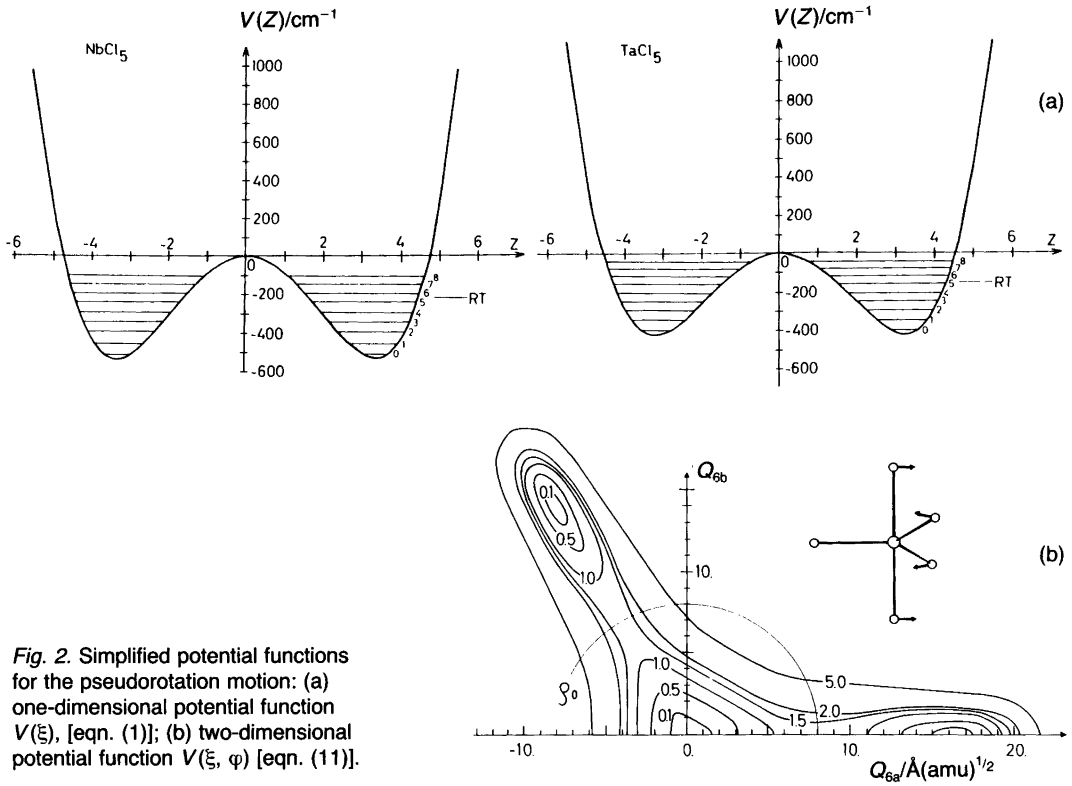

Fig. 2. Simplified potential functions for the pseudorotation motion: (a) one-dimensional potential function $V(\xi)$, [eqn. (1)]; (b) two-dimensional potential function $V(\xi, \varphi)$ [eqn. (11)].

symmetry point groups, e.g. D_{3h} or C_{4v}, is no longer valid. All 20 topological isomers are mutually interrelated by inversion-permutation operations.[62]

Following Ref. 63 we will use the notation (1,2) (3,4,5) (Fig. 3) to describe one of the topological isomers of an ML_5 molecule. The first parentheses correspond to axial substituents and the second parentheses to equatorial ones numbered clockwise. Ten out of a total of 20 isomers formed in successive permutations of atoms in ML_5 can then be represented by the scheme given in Fig. 3. The remaining 10 isomers are enantiomers of each of the ten isomers shown. The graph describing possible polytopic rearrangement paths can then be represented as a pentagondodecahedron (Fig. 4) where each vertex corresponds to one of the topologically related isomers.[63] According to this representation of the isomerization process, each isomer can be transformed to one of the three "nearest" isomers along pentagondodecahedron edges, all these transitions being equally probable.

What is the mechanism of nuclear motions in polytopic rearrangements? No reliable answer to this question has as yet been obtained in any of numerous experimental studies of five-coordinate compounds. The most valuable information on PES of five-coordinate molecules is, we believe, provided by quantum chemical calculations. The *ab initio* calculations of PES of five-coordinate compounds performed until now.[12,13,46,64-67] are indicative of pseudorotation being a multi-dimensional motion involving concerted variation of all the atomic spacings and bond angles along a minimum energy path on a PES. For all the pentahalide moledules, the minimum energy path corresponds to the mechanism suggested by Berry.[15] This conclusion follows from the observation that calculated PES barrier values along the reaction coordinate corresponding to Berry's mechanism are far below those for

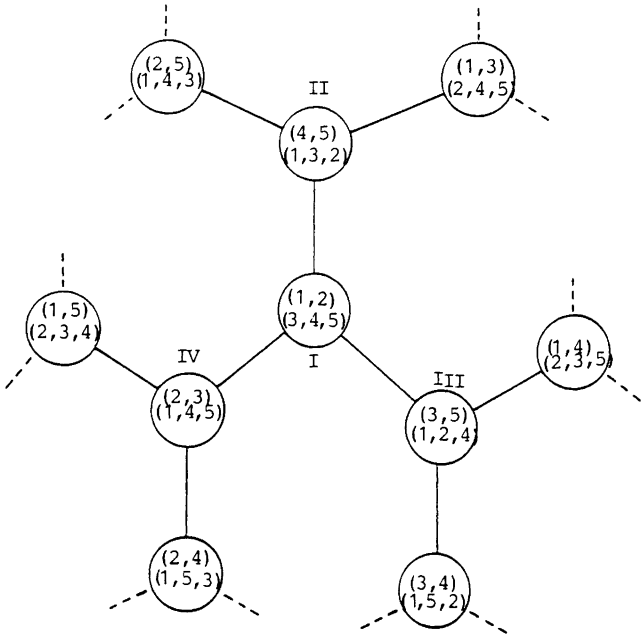

Fig. 3. Schematic representation of 10 of the total 20 topological isomers formed in successive permutations of atoms in ML_5 molecules.

other pseudorotation mechanisms such as turnstyle rotation,[68] tetrahedron edge crossing,[69–71] tetrahedral tunneling[72] and others[73,74] that can presumably be realized in rearrangements in complex five-coordinate compounds.

According to Berry's mechanism,[15] pseudorotation can involve simultaneous motion of axial and equatorial atoms to decrease the L_{ax}–M–L_{ax} angle from 180° to 120° and increase one of the L_{eq}–M–L_{eq} angles from 120° to 180° while atomic spacings vary as $r_{ax} \rightarrow r'_{eq}$ and $r_{eq} \rightarrow r'_{ax}$ (Fig. 1). It is assumed that the C_{4v} configuration is a saddle point of the PES describing pseudorotation if the trigonal-bipyramidal configuration corresponds to the PES minimum. The model potential function for pseudorotation, $V(\xi)$, can then be written in the form of eqn. (1) (Fig. 2). This potential function describes the transition between the first two nearest topological isomers (Figs. 3 and 4).

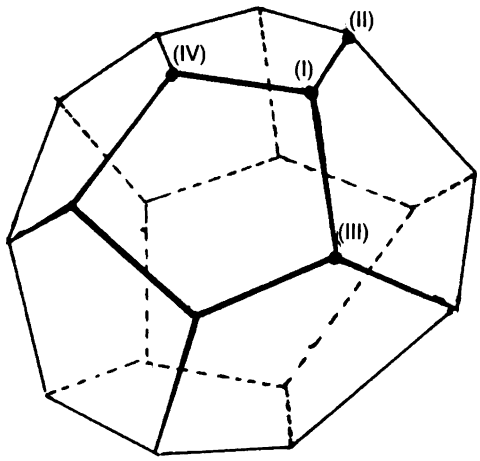

Fig. 4. The graph describing possible polytopic rearrangement paths.

We will further assume pseudorotation to be far slower than motions involving the other $(f-1)$ vibrational degrees of freedom ($f = 3N-6$, where N is the number of atoms in a molecule) and separate nuclear motions corresponding to pseudorotation from other molecular vibrations (the adiabatic approximation).

Electron diffraction intensity equation

According to Debye[75] the expression for the molecular contribution to scattering, $sM(s)_T$, can then be written as eqn. (2). Here the coordinates $q_1, q_2, \ldots, q_{f-1}$ correspond to $(f-1)$ normal vibrations and the coordinate ξ to pseudorotation.

$$sM(s)_T = \sum_{i \neq j=1}^{N} g_{ij}(s) \left\langle \frac{\sin sr_{ij}\,(q_1, q_2\,, \ldots\,, q_{f-1}, \xi)}{r_{ij}\,(q_1, q_2\,, \ldots\,, q_{f-1}, \xi)} \right\rangle \tag{2}$$

Separating intramolecular motion along ξ enables us to write

$$P(q_1, q_2\,, \ldots\,, q_{f-1}, \xi) = P_{\mathrm{fr}}(q_1, q_2\,, \ldots\,, q_{f-1} \mid \xi)\, P(\xi) \tag{3}$$

where $P_{\mathrm{fr}}\,(q_1, q_2\,, \ldots\,, q_{f-1} \mid \xi)$ is the probability density function describing skeleton vibrations and the coordinate ξ plays the role of a parameter. $P(\xi)$ is the pseudorotation probability density function. Eqn. (2) can then be rewritten in the form of eqn. (4), where the inner angular brackets mean the average over the normal coordinates $q_1, q_2\,, \ldots\,, q_{f-1}$. The probability density function along these coordinates can be approximated by the well-known eqn. (5),[76] where

$$sM(s)_T = \sum_{i \neq j=1}^{N} g_{ij}(s) \left\langle \left(\left\langle \frac{\sin sr_{ij}\,(q_1\,, \ldots\,, q_{f-1} \mid \xi)}{r_{ij}\,(q_1\,, \ldots\,, q_{f-1} \mid \xi)} \right\rangle_{q_i} \right) \right\rangle_{\xi} \tag{4}$$

$$P_{\mathrm{fr}}(q_1, q_2\,, \ldots\,, q_{f-1} \mid \xi) = \prod_{i=1}^{f-1} \left\{ 2\pi \langle q_i^2(\xi) \rangle^{1/2} \exp \left[- \frac{q_i^2(\xi)}{2\langle q_i^2(\xi) \rangle} \right] \right\} \tag{5}$$

$$sM(s)_T = \sum_{i \neq j=1}^{N} g_{ij}(s) \left\langle \exp[-s^2 \langle \Delta r_{ij}^2(\xi) \rangle / 2] \cdot r_{e,ij}^{-1}(\xi) \cdot \left\{ A_{ij}(s \mid \xi) \times \right. \right.$$

$$\left. \left. \sin [sr_{e,ij}(\xi)] + B_{ij}(s \mid \xi) \cdot \cos [sr_{e,ij}(\xi)] \right\} \right\rangle_{\xi} \simeq \sum_{i \neq j=1}^{N} \frac{g_{ij}(s)}{r_{e,ij}} \times$$

$$\left\langle \exp[-s^2 \langle \Delta r_{ij}^2(\xi) \rangle / 2] \left\{ A_{ij}^2(s \mid \xi) + B_{ij}^2(s \mid \xi) \right\}^{1/2} \cdot \sin \left[sr_{e,ij} + \arctan \frac{A_{ij}(s \mid \xi)}{B_{ij}(s \mid \xi)} \right] \right\rangle_{\xi}, \tag{6}$$

where:

$$A(s \mid \xi) \simeq 1 + \langle \Delta r^2(\xi) \rangle / r_e^2 - K(\xi)/r_e - s^2 \langle \Delta r^2(\xi) \rangle^2 / r_e^2$$

$$B(s \mid \xi) \simeq -s [\langle \Delta r^2(\xi) \rangle / r_e - K(\xi) + s^2 \langle \Delta r^2(\xi) \rangle \langle \Delta r(\xi) \rangle],$$

and $K(\xi)$ is given in Ref. 31, appendix I.

$$sM(s)_T \simeq \sum_{i \neq j=1}^{N} g_{ij}(s) \left[A_{ij}^2(s) + B_{ij}^2(s) \right]^{1/2} \cdot r_{e,ij}^{-1} \cdot \exp \left[-s^2 \left(\langle \Delta r_{ij}^2 \rangle_{\mathrm{fr}} + \langle \Delta r_{ij}^2(\xi) \rangle_{ps} \right) / 2 \right] \times$$

$$\sin s \left[r_{e,ij} + \langle \Delta r_{ij}(\xi) \rangle - \frac{s^2}{6} \left(\langle \Delta r_{ij}^3(\xi) \rangle - 3 \langle \Delta r_{ij}^2(\xi) \rangle \langle \Delta r_{ij}(\xi) \rangle + 3 \langle \Delta r_{ij}(\xi) \rangle^3 \right) \right] \tag{7}$$

the coordinates q_i depend parametrically on ξ.

Expanding $r_{ij}(q_1, q_2, \ldots, q_{f-1} \mid \xi)$ into a series in normal coordinates and integrating yields eqn. (6). As all the functions entering into eqn. (6) vary only slightly with ξ we can rewrite this equation in the form of eqn. (7), where $\langle \Delta r_{ij}^2 \rangle_{fr}$ is the skeleton vibrational amplitude, and

$$\langle \Delta r_{ij}^2(\xi) \rangle_{ps} = \langle \Delta r_{ij}^2(\xi) \rangle - \langle \Delta r_{ij}(\xi) \rangle^2 \quad (8)$$

As has been shown in the foregoing, the electron diffraction data on the pentahalides studied can be analyzed without taking quantum mechanical tunneling effects into consideration. In addition to that we have $\theta = hc\omega_7/kT < 1$ for all the molecules studied [$\omega_7(e')$ is the "pseudorotation frequency"]. The quantities $\langle \Delta r^n(\xi) \rangle$ in eqn. (7) can then to a good approximation be calculated using the formula

$$\Delta r^n(\xi) = \frac{\int \exp[-V(\xi)/RT]\, \Delta r^n(\xi)\, \alpha[\Delta r(\xi)]}{\int \exp[-V(\xi)/RT]\, \alpha[\Delta r(\xi)]} \quad (9)$$

that is by averaging over the classical probability density function.

As the function $sM(s)_T$ given by eqn. (7) is directly related to the pseudorotation potential function $V(\xi)$, an attempt can be made to determine the $V(\xi)$ function parameters and the equilibrium $r_{e,ij}$ parameters.

This approach resembles in a way the procedure suggested in Ref. 77 to account for internal rotation (see also Ref. 78 and references therein), and it has been realized in Ref. 51 in the study of $NbCl_5$ and $TaCl_5$ pentachlorides. An analysis carried out in this paper has enabled us to remove discrepancies between the experimental and theoretical intensity, $sM(s)$, and radial distribution, $f(r)$, curves arising from quasi-rigid molecular models of $NbCl_5$ and $TaCl_5$, and to determine the pseudorotation potential function, $V(\xi)$, parameters, [eqn. (1)]. Solving the Schrödinger equation with the pseudorotation potential function $V(\xi)$ found in the analysis of the electron diffraction data[51] yielded the "pseudorotation vibrational frequencies", $\omega_7(e')$, for $NbCl_5$ and $TaCl_5$. The calculation results are in good agreement with the spectroscopic values,[79–81] which proves the validity of the approximations made in deducing eqn. (7) and involved in the model of pseudorotation used to interpret electron diffraction data. Solving the Schrödinger equation for a one-dimensional potential function $V(\xi)$, however, gives a set of crowding vibrational levels whose energy is below the barrier height, V_0. For this reason the solution cannot explain all the specific features observed in the $\omega_7(e')$ band spectra of some pentahalides.[82–85] This shortcoming can be suggested to arise from ignoring equally probable polytopic rearrangement paths shown in Fig. 3 (or Fig. 4) corresponding to the permutations

$$\{(1,2)(3,4,5)\} \Leftrightarrow \begin{Bmatrix} (4,5)(1,3,2) \\ (3,5)(1,2,4) \\ (2,3)(1,4,5) \end{Bmatrix}$$

A suitable pseudorotation potential function including at least three nearest pseudorotation paths can be obtained by shifting the $V(\xi)$ function along the axis by ξ_0. The expression for $V(\xi)$ [eqn. (1)] then becomes

$$V(\xi) = V_0(\xi/\xi_0)^2[(\xi/\xi_0)^2 - 4(\xi/\xi_0) + 4] \quad (10)$$

As three equivalent pseudorotation PES minima are related to each other by rotations about the C_3 axis passing through the axial atoms, the potential function taking this feature of intramolecular rearrangement into account can be written (Fig. 2b) as:

$$V(\xi) = V_0(\xi/\xi_0)^2[(\xi/\xi_0)^2 - 4(\xi/\xi_0)\cos 3\varphi + 4] \quad (11)$$

where ξ and φ are the polar coordinates. We assume that pseudorotation can be described by a doubly degenerate normal coordinate $q_7(\xi, \varphi)$ (see also Ref. 51) with the components q_{7a} and q_{7b} related to the polar coordinates ξ and φ according to

$$q_{7a} = \xi \cos \varphi, \quad q_{7b} = \xi \sin \varphi.$$

The potential function $V(\xi, \varphi)$ [eqn. (11)] can then be rewritten in the form of eqn. (12) (see also Refs. 84 and 85).

$$V(q_{7a}, q_{7b}) = \tfrac{1}{2}a(q_{7a}^2 + q_{7b}^2)^2 + b(q_{7a}^2 + q_{7b}^2) - c(q_{7a}^3 - 3q_{7a}q_{7b}^2) \quad (12)$$

The potential function (11) parameters V_0 and ξ_0 are related to the potential function (12) parameters a, b and c by:

$$V_0 = a^3/32c^2, \quad \xi_0 = c/4b.$$

Potential function (12) has been shown[83–85] to give a satisfactory description of the vibrational spectra of PF_5, AsF_5 and VF_5.

An analysis of electron diffraction data based on the potential function (12) can be performed as described above. The values $\langle \Delta r^n(\xi) \rangle$ should now be calculated using the function $V(\xi, \varphi)$ and the equation:[86]

$$\langle \Delta r^n(\xi, \varphi) \rangle = \frac{\int_0^{\xi_0} \int_0^{2\pi} \Delta r^n(\xi, \varphi) \exp[-V(\xi, \varphi)/RT] \xi d\xi d\varphi}{\int_0^{\xi_0} \int_0^{2\pi} \exp[-V(\xi, \varphi)/RT] \xi d\xi d\varphi} \quad (13)$$

by numerical integration techniques.

The cumulant representation of the $sM(s)_T$ function,[31,87–90] obviating the necessity of using the simplified form for $sM(s)_T$ given by eqn. (7), can also be employed in an electron diffraction analysis of pseudorotation. The corresponding expression is given by eqn. (14) (see also Refs. 87 and 88). The latter equation for $sM(s)_T$ can be simplified from consideration of only a weak dependence of the functions $A(s \mid \xi, \varphi)$ and $B(s \mid \xi, \varphi)$ on the parameters (ξ, φ), and using the adiabatic approximation that allows separation of motions along the non-rigid coordinates q_{6a} and q_{6b} from other intramolecular vibrations. An analysis of electron diffraction data can then be performed as follows:

The first four cumulants (the so-called excess approximation) will be used in expansions (17) and (18) (Refs. 87 and 88). As follows from the analysis carried out in the foregoing, they give a sufficiently good representation of the probability density function describing the distribution of internuclear distances in an ensemble of molecules.

The cumulant averages are calculated from the eigenvectors and eigenvalues of the harmonic vibrational matrix of a molecule. These are obtained in terms of symmetry coordinates using the generalized valence force field (GVFF) formalism. the GVFF parameters are estimated from spectroscopic vibrational frequencies and vibrational amplitudes[31] determined by conventional procedures at a preliminary stage. Furthermore, eigenvectors are not refined, for as has been shown in Ref. 91, they depend only very slightly on uncertainties in force-field parameters. The electron diffraction structural and dynamical problem is solved using equilibrium internuclear distances $r_e(M–L_{ax})$ and $r_e(M–L_{eq})$ (or

$$sM(s)_T = \sum_{i \neq j=1}^{N} \frac{g_{ij}(s)}{r_{e,ij}} \left\langle \exp[Q_{ij}(s \mid \xi, \varphi)] \left\{ A_{ij}(s \mid \xi, \varphi) \cdot \sin[sr_{e,ij} + P_{ij}(s \mid \xi, \varphi)] + B_{ij}(s \mid \xi, \varphi) \cdot \cos[sr_{e,ij} + P_{ij}(s \mid \xi, \varphi)] \right\} \right\rangle \quad (14)$$

where:

$$A(s \mid \xi, \varphi) = 1 - P'(s \mid \xi, \varphi)/r_e - {}^1/_{r_e^2}\{[Q'(s \mid \xi, \varphi)]^2 + Q''(s \mid \xi, \varphi) - [P'(s \mid \xi, \varphi)]^2\} \quad (15)$$

$$B(s \mid \xi, \varphi) = Q'(s \mid \xi, \varphi)/r_e - {}^1/_{r_e^2}[2Q'(s \mid \xi, \varphi)\, P'(s \mid \xi, \varphi) + P''(s \mid \xi, \varphi)] \quad (16)$$

$$P(s \mid \xi, \varphi) = \sum_{n=0}^{\infty} \frac{i^{2n} s^{2n+1}}{(2n+1)!} \langle \Delta r^{2n+1}(\xi, \varphi) \rangle_c \quad (17)$$

$$Q(s \mid \xi, \varphi) = \sum_{n=0}^{\infty} \frac{(is)^{2n}}{(2n)!} \langle \Delta r^{2n}(\xi, \varphi) \rangle_c \quad (18)$$

Δr_{ax-eq}), and also V_0 and ξ_0 as independent parameters. The parameters are refined using the minimization algorithm proposed in Ref. 92. The present analysis procedure is described in more detail in Refs. 31 and 88. The results obtained for various ML_5 molecules are given in the following section. It should be noted that various techniques for including pseudorotation in the analysis of electron diffraction data give geometrical and potential function parameter values for the pentahalides studied which coincide within the experimental uncertainties. Therefore, from the practical point of view, the technique based on eqn. (7) for $sM(s)_T$ should be recommended as the simplest and most convenient one. The technique based on the scattering intensity function, $sM(s)_T$ [eqn. (14)], is somewhat tedious to employ. However, in principle eqn. (14) can be expected to give sufficiently accurate molecular parameter values.[88]

Results of gas-phase electron diffraction studies of pentahalides

In this section, with the exception of the results for PF_5, which is a convenient test example for testing the data analysis procedure, the experimental results obtained at Moscow University in cooperation with the Oslo University electron diffraction group are reviewed.

Phosphorus pentafluoride. The experimental data of Ref. 30 have been used in our analysis.

The technique based on eqn. (7), with a two-dimensional potential function $V(\xi, \varphi)$ given by eqn. (11), yields a barrier to pseudorotation of $V_0 = 1193(245)$ cm^{-1}.[31,87] These results are in agreement with the high-resolution Raman spectroscopy data on PF_5[84,85] (see Table 1) and also *ab initio* results: V_0 = 1329 cm^{-1} [64] and V_0 = 1337.5±167.2 cm^{-1}.[66] The pseudorotation transition state geometry (symmetry C_{4v}) found from the ξ_0 value obtained in our analysis is characterized by a 101° angle made by the apical and basal bonds. According to the quantum-mechanical calculations,[64,66,93–99] this angle is predicted to be 99–103°.

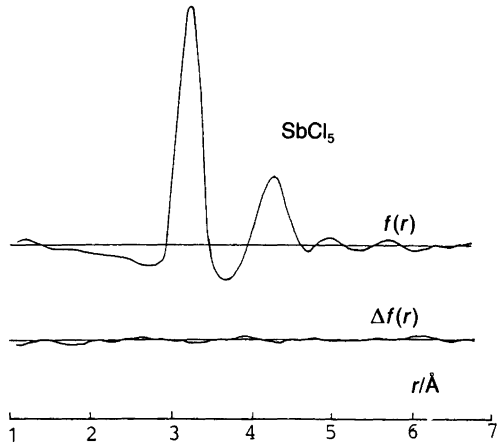

Fig. 5. Radial distribution curve for $SbCl_5$.

The equilibrium r_e^{ax} and r_e^{eq} distances compare well with those cited in Ref. 100, where the technique suggested in Ref. 101 was employed in a combined analysis of high resolution vibration-rotational spectra[102,103] and electron diffraction data.[100]

The good agreement between the results of the investigation referred to above and the results of the cited studies (see also Table 1) indicates that the technique suggested to include pseudorota-

Table 1. Molecular parameters of the Group V pentahalides (D_{3h} symmetry of the equilibrium configuration).

Parameter	PF_5		$SbCl_5$	$NbCl_5$	$TaCl_5$	$TaBr_5$	
	Ref. 87	Ref. 100	Ref. 104	Ref. 51	Ref. 51	Ref. 86	
r_e^{ax}/Å	1.576(4)	1.576(4)	2.338(7)	2.338(7)	2.369(4)	2.469(8)	2.467(8)[c]
r_e^{eq}/Å	1.530(3)	1.529(3)	2.277(5)	2.241(4)	2.227(3)	2.417(4)	2.414(4)
V_0/cm^{-1}	1193(245)	1139 – 995[a]	665(210)	524(245)	420(210)	490(210)	455(210)
∠ ($L_a M L_b$)/° for C_{4v} configuration	101(3)	103 – 99[b]	101(2)	104(5)	104(3)	99(7)	99(7)

[a]Refs. 84 and 85. [b]Refs. 64, 66 and 93–99. [c]The data obtained are based on eqn. (7).

tion in electron diffraction investigations is applicable.

Antimony pentachloride. The study on $SbCl_5$[104] has confirmed the earlier conclusion[105] of its trigonal bipyramidal structure. The radial distribution curve is shown in Fig. 5. In Ref. 105 the average r_a(Sb–Cl) distance was found to be 2.26 Å. This value differs substantially from the more recent one of 2.302 Å. The latter result fits the X-ray data on $SbCl_5$ better,[106] $r(Sb–Cl_{ax})$ = 2.34 Å, $r(Sb–Cl_{eq})$ = 2.29 Å and hence, $r(Sb–Cl)_{av}$ = 2.31 Å.

The barrier to pseudorotation found for $SbCl_5$ in Ref. 104, viz. 665(210) cm^{-1}, can be compared with estimates obtained in other studies. Use of the harmonic potential functions for the low-frequency $SbCl_5$ vibrations gives barrier values of 3288 and 3113 cm^{-1}.[107,108] The value of 769 cm^{-1} cited in Ref. 109 has been obtained by multiplying 3113 cm^{-1} by an empirical factor of 0.25. This coefficient was obtained by comparing values for the barrier to pseudorotation for VF_5 found using a harmonic potential function[108] and calculated from the low-frequency Raman spectrum of VF_5.[110]

Niobium and tantalum pentachlorides. The radial distribution curves for $NbCl_5$ and $TaCl_5$ are given in Fig. 6. The average (M–Cl) distances in $NbCl_5$ and $TaCl_5$ found in Ref. 51 agree well with the results of the earlier investigations.[111–113] The average r_e(Nb–Cl) distance, 2.280(3) Å, is very close to r_e(Ta–Cl) = 2.284(2) Å, which can be explained by the lanthanide contraction effect. The differences between the axial and equatorial spacings, Δr_{ax-eq}, are 0.097(9) and 0.142(5) Å for $NbCl_5$ and $TaCl_5$, respectively. The values are close to Δr_{ax-eq} for PCl_5, $0.10_4 \pm 0.01$ Å[32] and somewhat larger than the values for PF_5 and AsF_5.[114]

A comparison of the Δr_{ax-eq} values found for $NbCl_5$ and $TaCl_5$ shows that the equatorial distance in $NbCl_5$ is longer than that in $TaCl_5$ by 0.014(5) Å, whereas the axial Nb–Cl distance is shortened by 0.031(7) Å. An increased stability, with increase in atomic number, of valence state III compared with V is explained by relativistic effects on atomic electronic structures.[115] The observed differences in equatorial/axial bond lengths for $NbCl_5$ and $TaCl_5$ are probably a further manifestation of these effects.

In the solid state, $NbCl_5$ exists in a dimeric form[116,117] containing bonds of three types: equatorial, $r(Nb–Cl_{eq})$ = 2.250(6) Å, axial, $r(Nb–Cl_{ax})$ = 2.302(5) Å, and bridged, $r(Nb–Cl_b)$ = 2.555(6) Å. Tantalum pentachloride is isomorphic with niobium pentachloride.[116,117] In the gas phase, $NbCl_5$ and $TaCl_5$ exist as monomeric species,[118,119] like PF_5, $SbCl_5$[112,119] and $TaBr_5$.[120]

The barrier to pseudorotation determined in Ref. 51 is close to the value found earlier for VF_5,[84,85] viz. 523 – 428 cm^{-1}. The angle between the apical and basal bonds is 104(3)°, in agree-

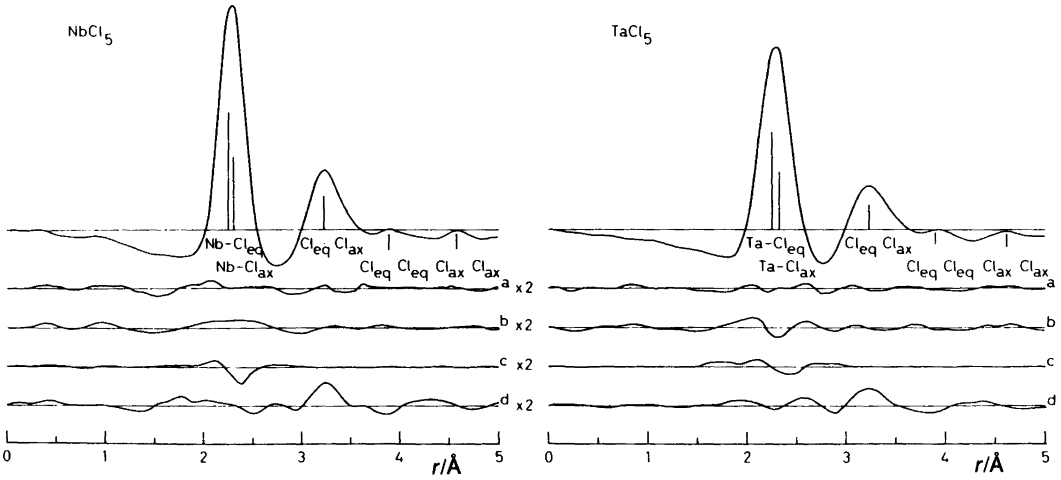

Fig. 6. Radial distribution curve for (a) $NbCl_5$ and (b) $TaCl_5$.

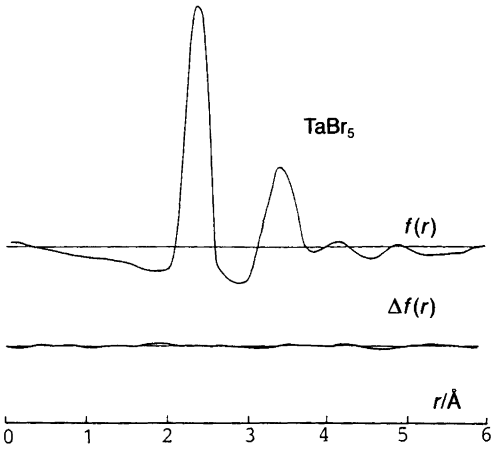

Fig. 7. Radial distribution curve for $TaBr_5$.

ment with the *ab initio* results[65] for a number of transition element complexes; for example, the L_a–M–L_b angle was calculated to be 106° in VF_5 and 105° in $Fe(CO)_5$.

Tantalum pentabromide. The electron diffraction study reported in Ref. 86 has confirmed the earlier conclusions for a trigonal bipyramidal structure, viz. $TaBr_5$.[111,121] the radial distribution curve for $TaBr_5$ is shown in Fig. 7. The average bond length, r_a(Ta–Br) = 2.446(8) Å,[86] is in good agreement with the results obtained in the earlier studies, viz. 2.45(3) Å[111] and 2.44(2) Å.[121] The Δr_{ax-eq} value of 0.062 Å is somewhat smaller than in the pentachlorides $NbCl_5$ and $TaCl_5$. The barrier to pseudorotation in $TaBr_5$, V_0 = 490(210) cm^{-1}, is close to those for $NbCl_5$ and $TaCl_5$. A strong correlation between the parameters V_0 and ξ_0, observed in Ref. 86, increases with decreasing barrier height.

Multiple intramolecular scattering effects. The contribution from multiple (triatomic) scattering to the molecular scattering intensity, $sM(s)_T$, has been calculated using the procedure suggested in Refs. 122 and 123. An analysis shows that triatomic scattering effects result in decreasing Δr_{ax-eq} and increasing r_e(M–Cl_{eq}) for $SbCl_5$, $NbCl_5$, $TaCl_5$ and $TaBr_5$.[51,86] Radial distribution difference curves obtained in refinements of molecular structures with and without taking triatomic scattering effects into consideration have a form which resembles that of a Fourier transform of triatomic scattering intensity (Figs. 5 to 7). Ignoring triatomic scattering also results in somewhat larger deviations of theoretical molecular scattering intensity from experimental ones.[51,86] Thus, the R_f value increases from 7.9 to 9.0 % for $NbCl_5$ and from 7.7 to 8.8 % for $TaCl_5$.[51] Therefore, triatomic scattering has a certain effect on pentahalide molecular parameters, and taking multiple scattering effects into consideration to a certain extent improves the agreement between experimental and theoretical intensity and radial distribution curves.

Discussion of results on pentahalides

Our studies of pentahalide molecules yielded the parameters of the potential function $V(\xi, \varphi)$ [eqn. (11)] which describes Berry pseudorotation arising as a result of thermal excitation of the low-frequency $\omega_7(e')$ vibration. It would be of interest to compare the vibrational transitions calculated for the potential functions determined by us with the experimental data. We have estimated the fundamental frequencies for $SbCl_5$, $NbCl_5$, $TaCl_5$ and $TaBr_5$ using the one-dimensional pseudorotation potential function $V(\xi)$, [eqn. (1)]. To do this we employed the tables given in Ref. 124 for the potential functions of the type

$$V(Z) = A[Z^4 - BZ^2] \qquad (19)$$

where

$$A = (\hbar^2/2\mu)^{2/3}a^{1/3},\ B = (2\mu/\hbar^2)^{1/2}a^{-2/3}b,$$

$$Z = (2\mu/\hbar^2)^{1/6}a^{1/6}\xi,\ a = V_0/\xi_0^4,\ = 2V_0/\xi_0^2,$$

μ is the reduced pseudorotation mass[$\mu \approx (\mathbf{G}^{-1})_{77}$], and $\mathbf{G}$ is the matrix of kinematic coefficients for the ML_5 molecule.

The V_0 and ξ_0 values determined for $SbCl_5$, $NbCl_5$, $TaCl_5$ and $TaBr_5$ have been used to calculate the $\Delta E_{0\leftarrow1}/hc$ quantities, which were found to be 60,[104] 55, 50[51] and 39 cm^{-1},[86] respectively. Experimentally, the corresponding vibration is observed at 58, 54, 70[80] and 79 cm^{-1}.[81] The two sets of values compare well, except for $TaBr_5$.

Note that in the series TaF_5, $TaCl_5$ and $TaBr_5$, all the frequencies decrease monotonically (see e.g. Ref. 125) except for $\omega_7(e')$, which is substantially higher for $TaBr_5$ than for $TaCl_5$. There

are, therefore, some reasons to believe that in Refs. 80 and 81 a "hot" band corresponding to the $\omega_7(e')$ vibration probably has been observed.

As has already been mentioned, we cannot explain all the specific features of the $\omega_7(e')$ band spectra of PF_5, AsF_5 and VF_5[84,85] if we solve the Schrödinger equation using a one-dimensional potential function $V(\xi)$ [eqn. (1)]. This is an obvious indication of the necessity of employing the two-dimensional $V(\xi, \varphi)$ function defined by eqn. (11).

The variation procedure suggested in Refs. 126 and 127 has been applied to solve the Schrödinger equation for the $V(\xi, \varphi)$ function transformed to the form $V(q_{7a}, q_{7b})$ [eqn. (12)]. The anharmonic vibrational Hamiltonian is then written in the form

$$\hat{H}_{\text{vib.}} = -\hbar^2/2 \sum_{i,j} t(q)^{1/4} \frac{\partial}{\partial q_i} \tau(q)_{ij} \cdot t(q)^{-1/2} \frac{\partial}{\partial q_i} t(q)^{1/4} + V(q) \qquad (20)$$

where the q_i's are the internal vibrational coordinates, the $\tau(q)_{ij}$'s are the elements of the matrix of kinematic coefficients which depend on the vibrational coordinates, and $t(q)$ is the determinant of that matrix.

For the potential function $V(q)$ all the vibrations except for q_7 were assumed to be harmonic. Thus, the coordinates corresponding to $(f-1)$ degrees of freedom were separated from q_7. The wave function of the vibration q_6 was chosen as a linear combination of the two-dimensional harmonic oscillator wave functions:

$$\Psi_n(q_{7a}, q_{7b}) = \sum_{i,j} c_{ij} \chi_i^{(n)}(q_{7a}) \chi_j^{(n)}(q_{7b}) \qquad (21)$$

where $\{\chi\}$ is the set of one-dimensional harmonic oscillator wave functions:

$$\chi^{(n)}(q) = \exp(-\lambda/2\, q^2)\, H_n(\lambda^{1/2} q) \qquad (22)$$

and $H_n(\lambda^{1/2}q)$ are the Hermite polynomials; $n = 0,1,2,\ldots$.

The constants λ in eqn. (22) can be determined from the standard solution for a harmonic oscillator with the potential function $V(q_{7a}, q_{7b})$ [eqn. (12)], where the parameters b and c are set at zero. It is, however, more convenient to optimize λ in the course of a variation procedure simultaneously with the coefficients c_{ij}. It has been shown in Ref. 86 that low-frequency vibrational states converge with a 0.1–0.2 cm^{-1} accuracy within the summation range of $0 \leq i, j \leq 16$. This very range has been used in the final calculations. The obtained frequencies and their symmetry assignments are given in Table 2 for $V_0 = 490\ cm^{-1}$. Since the uncertainty in V_0 was estimated to be 210 cm^{-1},[86] calculations have also been performed for the boundary V_0 values. The frequency values then show systematic shifts within $\pm 25\,\%$, while the characteristic features of the spectra remain unaffected. The correlation diagram of the energy levels is represented in Fig. 8. It can be seen that the experimental frequency at 70, 80 or 79 cm^{-1} [81] can be assigned as the $a_1' \rightarrow a_1'$ transition of $83 \pm 21\ cm^{-1}$ energy which appears to be active in the IR absorption spectrum. The data in Table 2 show that the calculated $a_1' \rightarrow e'$ transition frequency, $42 \pm 10\ cm^{-1}$, is close to the value of 39 cm^{-1} obtained for the one-dimensional potential function $V(\xi)$, [eqn. (1)]. Therefore one need not necessarily use a rather cumbersome variational procedure to solve the Schrödinger equation for the two-dimensional potential function: for practical purposes such as calculations of thermodynamic functions, the $\omega_7(e')$ frequency can be simply estimated using the one-dimensional potential function and the tables of Ref. 124.

Table 2. The vibrational frequencies for $q_7(e')$ vibrations (cm^{-1}).

V	
0	42 (e')
1	83 (e'), 85 (e')
2	124 (e'), 128 (a_1'), 129 (a_2')
3	163 (a_1'), 165 (e'), 172 (e')

To summarize, a trigonal-bipyramidal equilibrium configuration with axial bonds elongated relative to equatorial ones has been determined for all the pentahalide molecules studied. According to the results of numerous X-ray diffraction studies of trigonal-bipyramidal five-coordinate compounds of the general formula ML_5 the $r(M\text{–}L_{ax})/r(M\text{–}L_{eq})$ ratios fall within the range of 1.03 to 1.07.[20] With molecules studied by electron

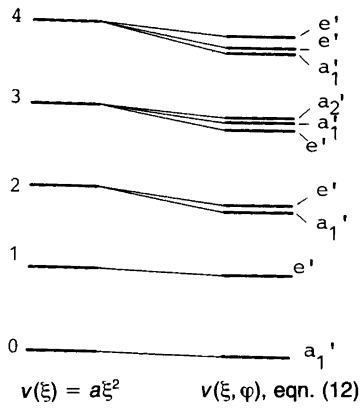

Fig. 8. Correlation diagram for the vibrational energy levels of the two-dimensional isotropic harmonic oscillator and two-dimensional potential function $V(\xi, \varphi)$, [eqn. (12)].

diffraction, this range is 1.03 to 1.05 (Table 1).

There are certain specific features of pseudorotation which are characteristic of all the compounds studied. For VF_5, $NbCl_5$, $TaCl_5$ and $TaBr_5$, the amplitudes of vibration calculated on the basis of the harmonic approximation differ strongly from those observed experimentally. For PF_5, AsF_5 and $SbCl_5$, the differences are less or not at all significant. This can be explained by different vibrational level populations at the electron diffraction experiment temperatures, as is illustrated by Fig. 9. In VF_5, $NbCl_5$, $TaCl_5$ and $TaBr_5$, sub-barrier levels have comparable and over-barrier ones only low populations. In PF_5 and $SbCl_5$, high populated levels lie substantially below the barrier to pseudorotation. At the same time, intramolecular motions along the polytopic rearrangement coordinate are strongly anharmonic, which results in a considerable asymmetry of the probability density function peaks, first and foremost in those corresponding to the $r(L_{eq} \ldots L_{eq})$ and $r(L_{eq} \ldots L_{ax})$ distances. It appears that the over-barrier pseudorotation mechanism is realized in all the pentahalide molecules studied by gas-phase electron diffraction.

The uncertainties in the calculated barrier heights are fairly large. In addition to this the quantities V_0 and ξ_0 are weak parameters, and they therefore depend critically on systematic experimental errors and on a number of electron scattering effects that, at present, are difficult to take into account adequately, such as multiple intermolecular scattering,[129] chemical bonding,[130] errors involved in the tabulated scattering amplitudes,[131] etc. Inadequacy of the pseudorotation potential function models, inaccuracy of experimental vibrational frequencies not corrected for anharmonicity, approximations inherent in separating pseudorotation from frame vibrations, and an inadequate treatment of anharmonicity of frame vibrations should also be taken into consideration. Nevertheless, the pseudorotation model employed has enabled us to improve the agreement between experimental and theoretical curves. For $NbCl_5$, $TaCl_5$ and $TaBr_5$, we have also been able to reduce the difference between the theoretical and experimental amplitude values, for the latter are far larger than those calculated using the harmonic approximation. It is important that better fits are obtained with a smaller number of variables: cf. the requirement of 7

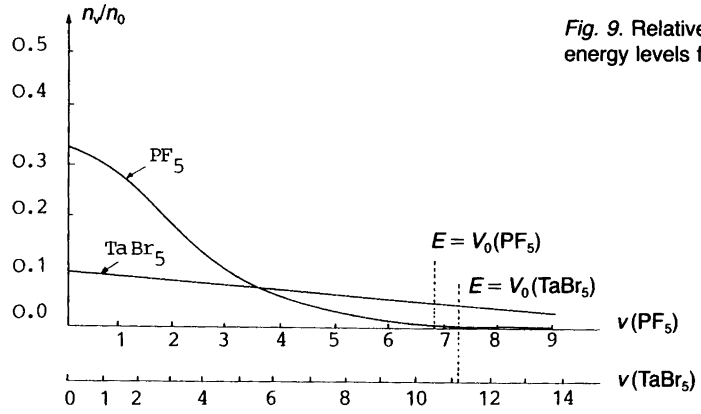

Fig. 9. Relative populations of the $\omega_7(e')$ vibrational energy levels for PF_5 and $TaBr_5$ molecules.

parameters in the conventional procedure (two geometrical, r_a^{ax} and r_a^{eq} or Δr_{ax-eq} and five vibrational ones, l_{ax}, l_{eq}, $l_{eq\ldots eq}$, $l_{ax\ldots ax}$ and $l_{eq\ldots ax}$) as opposed to 4 in the present procedure (r_e^{ax}, r_e^{eq}, V_0 and ξ_0).

B. Molecular structures of oligomeric pentafluorides

Background

Three structure types are realized in solid pentafluorides[132–135] (Fig. 10). These can contain tetrameric molecules with (–MF_6–) units linked by either linear (NbF_5, MoF_5, TaF_5)[136] (Fig. 10a) or angular (M–F_6–M) bridged (RuF_5, RhF_5, OsF_5, IrF_5, PtF_5)[137] (Fig. 10b), or by zigzag chains of (–MF_6–) units with bridging *cis* fluorine atoms (VF_5, CrF_5, TcF_5, ReF_5)[138] (Fig. 10c).

X-Ray diffraction studies of NbF_5 and TaF_5 single crystals[136] have shown the compounds to form monoclinic crystals having space group $C2/m$, $Z = 8$. The basic structure units are tetrameric $(MF_5)_4$ molecules of D_{4h} symmetry. Each metal centre has a distorted octahedral environment of six fluorine atoms (Fig. 10). Octahedral fragments are linked by bridging *cis* fluorine atoms, and the metal atoms form a near regular square. Unlike niobium and tantalum pentafluorides, where all the four M–F_B–M angles are identical,[136] antimony pentafluoride tetramer contains two pairs of angles of 141 and 170°[139] (Fig. 10a).

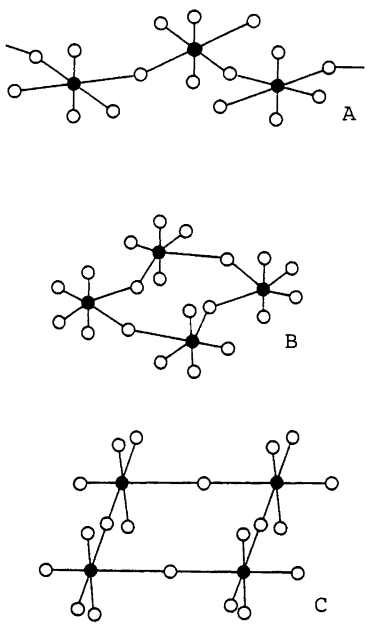

Fig. 10. Basic structural types for the pentafluorides in the condensed phase. (a) Structural type of NbF_5, MoF_5 and TaF_5. (b) Structural type of RuF_5, RhF_5, OsF_5, IrF_5 and PtF_5. (c) Structural type of VF_5, CrF_5, TcF_5 and ReF_5.

A comparative analysis of the Raman spectra of gold(V)[140,141] and other transition metal pentafluorides shows that AuF_5 can contain linear bridges in a manner similar to α-UF_5,[142] although no definite conclusions concerning the crystal structure of AuF_5 can be drawn. Non-equivalence of fluorine atoms in AuF_5 is verified by the observation of quadrupole splitting in the ^{197}Au Mössbauer spectrum.[141]

According to spectroscopic data,[142–149] oligomeric $(MF_5)_n$ units are also present in molten niobium, tantalum and antimony pentafluorides over a wide temperature range.

The first study that reliably established the presence of oligomeric metal pentafluoride molecules in the gas phase was the electron diffraction investigation of NbF_5 and TaF_5.[150,151] A comparison of the theoretical and experimental molecular intensity and radial distribution curves led the authors[150,151] to conclude that the gas phase mainly consisted of tetrameric species having a structure similar to that characteristic of the crystalline compounds[136] (Fig. 10a). A certain amount of disagreement between the experimental and theoretical radial distribution curves for tetramers in the region of 4 to 6 Å was observed for NbF_5, but not for TaF_5. Nevertheless, the authors claimed both compounds to have the same structure and gas-phase molecular composition, and attributed the poor fit for niobium pentafluoride to insufficiently accurate measurements in the corresponding region.[150,151]

The data of Refs. 150–160 show that oligomeric metal pentafluoride molecules are characterized by very high thermal stability. This follows in particular from the presence of considerable amounts of oligomers even in vapours overheated by 100 to 150 °C. Thus, electron diffraction patterns obtained in Ref. 151 at overheatings of ~ 100 °C correspond to superposition

of scattering from monomer and polymer molecules, and the 757 (NbF_5) and 752 cm^{-1} (TaF_5) absorption bands corresponding to the polymers are still sufficiently strong at a 150° overheating. According to the electron diffraction data,[153,154] NbF_5 and TaF_5 vapours require overheating by ~340–400 °C in order for the oligomers to be fully dissociated to the monomeric species NbF_5 and TaF_5.

The procedure for electron diffraction data analysis

An electron diffraction study of the structure and intramolecular motions of polyatomic molecules under the conditions of a complex and unknown gas-phase composition and in the absence of sufficient data on molecular force fields is a difficult and often impracticable task, since solving the structural and vibrational problems then requires the determination of a large number of geometric and vibrational parameters. This is characteristic of all ill-posed problems (see, e.g. Refs. 161–163). Handling such problems requires the use of regularization algorithms which limit the ranges of admissible structure and vibrational parameter values. One of the possible approaches is the use of spectroscopic information on the system under investigation. An analysis of data in the literature (see Background, above), however, shows that spectroscopic data on oligomeric metal pentafluoride moledules are far from being complete.

In fact, for trimeric $(MF_5)_3$ molecules of D_{3h} symmetry (Fig. 11a), the total number of vibrational degrees of freedom is $3N-6 = 48$. Their distribution over the vibrational modes is determined by the representation:[164]

$$\Gamma = 6A_1'(R) + 2A_1'' + 4A_2'' + 4A_2'(IR) + 10E'(IR,R) + 6E''(R)$$

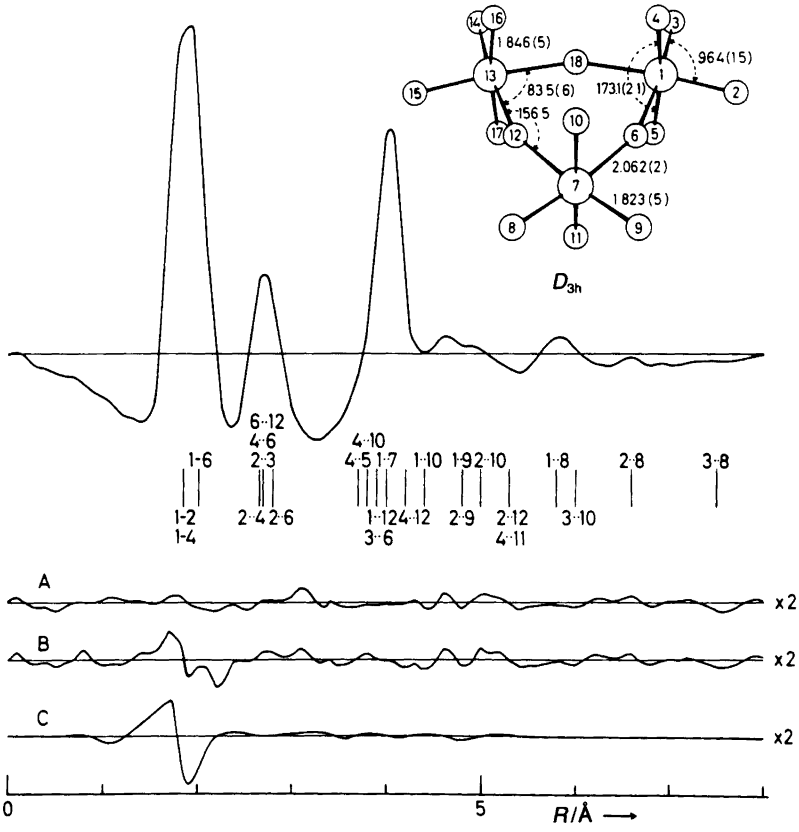

Fig. 11. Radial distribution curve and geometry of $(TaF_5)_3$.

The vibrations of A_1'' and A_2'' symmetry types are optically inactive. It follows from this consideration that the trimeric molecules of D_{3h} symmetry should give 14 IR and 22 Raman frequencies. The A_1'' and A_2'' frequencies can, in principle, be determined from combination modes. An analysis of data in the literature, however, shows that with metal pentafluorides, this is an exceedingly difficult problem. Therefore the spectroscopic information available is also insufficient to determine the force field of a molecule (see, e.g. Refs. 165–166).

The problem can be tackled on the basis of a potential function describing both electron diffraction and spectroscopic data. This approach implies the use of vibrational amplitude and shrinkage values[167–169] calculated using spectroscopic vibrational frequencies. Within this approach, a combined analysis can be carried out as follows.

A starting approximation to the valence force field of a molecule is chosen to obtain the force field in symmetry coordinates.[76] The latter is used to calculate the matrix of eigenvectors **L**, relating the symmetry coordinates to the normal coordinates. Further, the normal vibration frequencies are calculated, and the calculated frequencies are replaced by the experimental ones. The experimental frequencies and the matrix **L** are used to determine the amplitudes l and the shrinkage correction (D quantities) relating the distances r_a and r_α:[169]

$$r_\alpha = r_a + l^2/r - K = r_a + D = r_e + \langle \Delta z \rangle$$

where $K = (\langle \Delta x^2 \rangle + \langle \Delta y^2 \rangle)/2r$ is the correction for perpendicular motion.[76,168,169] The D and l quantities thus obtained are employed as starting approximations in the electron diffraction refinement of the r_α structure of a molecule.

If the treatment of scattering intensities gives amplitudes substantially different from those calculated using spectroscopic data, the valence force field parameters are refined and the whole calculation is recycled until satisfactory agreement between the spectroscopic and electron diffraction amplitude values is reached. This procedure seems to only slightly regularize the spectroscopic problem. Its practical use, however, shows that it enables the ambiguity of the electron diffraction problem to be reduced substantially. This is so because electron diffraction data are far less sensitive to uncertainties in the force field parameters than are spectroscopic data.

The use of this structural analysis technique has enabled us to determine the molecular structure and gas-phase compositions for antimony,[170] niobium,[170] tantalum[171] and gold pentafluorides[172], and molybdenum pentachloride.[173] More recently a similar procedure was applied to analyze the electron diffraction data on niobium,[174] molybdenum[175] and ruthenium[176] pentafluorides.

As with the monomeric pentahalides (see Part A, above), the harmonic approximation is probably inadequate to describe all types of intramolecular motions in these systems, and large-amplitude motions, such as six-membered ring deformations in $(MF_5)_3$ trimers (Fig. 11) and motions of non-bonded fluorine atoms attached to different metal atoms are likely to be important. With complex molecular structures, the determination of weak potential function parameters is, however, an exceedingly difficult task. Precisely this circumstance made necessary the use of the harmonic approximation in analysing electron diffraction data on vapours of an unknown composition.

Niobium and tantalum pentafluorides

Electron diffraction patterns for vapours over niobium and tantalum pentafluorides (and other compounds studied in Refs. 170–172 were obtained using a modified electron diffraction unit[177] at temperatures of 60(3) and 20(2) °C, respectively. The experimental details are given in Refs. 170 and 171. Applying the procedure described above and using the vibrational frequencies measured for gaseous niobium and tantalum pentafluorides[152] has revealed that the electron diffraction data can best be described in terms of a trimeric $(MF_5)_3$ model of D_{3h} symmetry (Figs. 11 and 12). The model involves 28 geometrical parameters including 24 internuclear distances and 4 valence angles. Independent parameters employed in the analysis were $r_\alpha(M–F_{ax})$, $\Delta r = r_\alpha(M–F_{ax}) - r_\alpha(M–F_t)$, $r_\alpha(M–F_b)$, $\angle_\alpha(F_{ax}–M–F_{ax})$, $\angle_\alpha(F_t–M–F_t)$, $\angle_\alpha(F_b–M–F_b)$ and $\angle_\alpha(M–F_b–M)$. All the 24 amplitudes corresponding to 24 types of interatomic distances were divided into 5 groups. The first group included the five shortest F···F distances. The mean amplitudes for the distances (1···8), (1···9), (1···12), (2···7), (2···13) and (6···13) (Fig. 11) made up the sec-

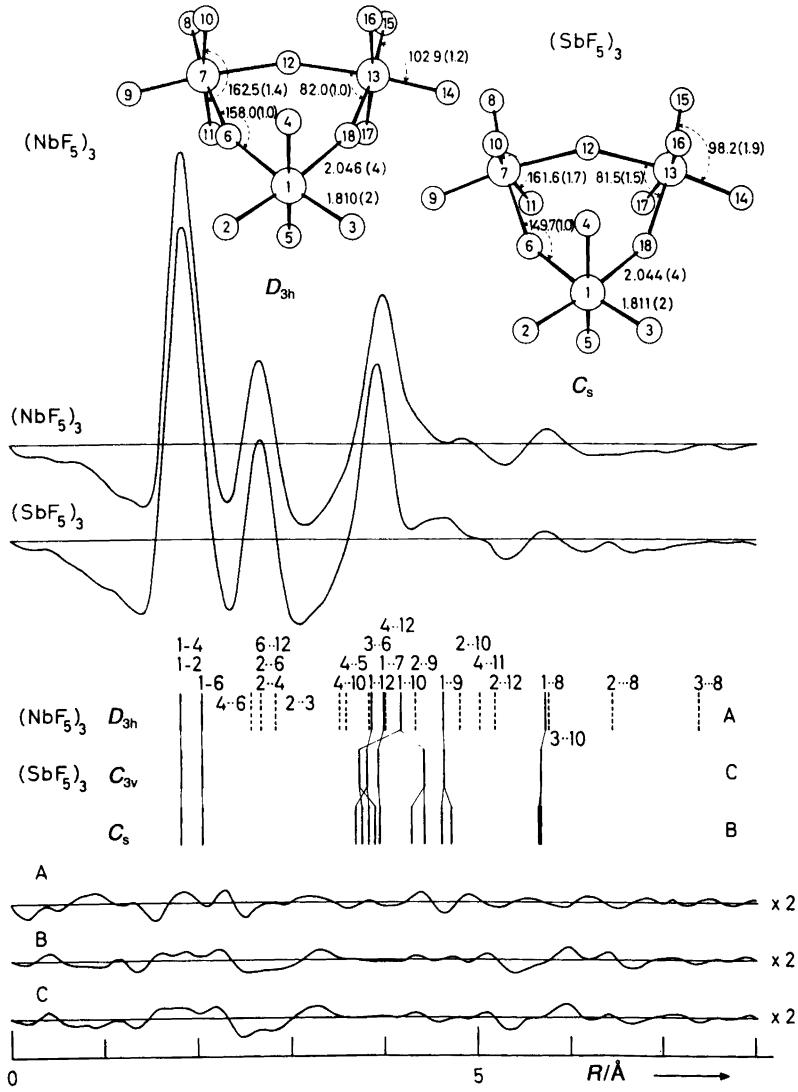

Fig. 12. Radial distribution curves and geometries of $(NbF_5)_3$ and $(SbF_5)_3$.

ond group, the (1 ··· 10) and (5 ··· 7) distances the third one, and the fourth group included the amplitudes for the (1 ··· 11) and (4 ··· 7) distances. The six amplitudes for the longest distances were combined into the fifth group.

The theoretical intensity functions were calculated with triatomic scattering effects included,[123] which can be expected to influence the structure parameters of $(MF_5)_3$-type molecules significantly. Only triatomic scattering from triangles including at least one metal atom and not containing angles above 170° was included. This gave 1782 triangles, of which 104 were different, out of the total of 4856 = $N(N-1)$ $(N-2)$ triple sum terms. The results obtained using the minimization procedure[178,179] are given in Table 3.

We were only able to determine the average distance $r_\alpha(M\text{–}F) = r_\alpha(M\text{–}F_{ax}) = r_\alpha(M\text{–}F_t)$ for $(NbF_5)_3$, the splitting parameter, Δr_{ax-t}, being found to be 0.001(14) Å, i.e. to involve an uncertainty exceeding the parameter value itself. Its introduction resulted in only an insignificant im-

Table 3. Geometrical parameters of the pentafluorides in the gas phase.[a]

Parameter	Nb_3F_{15}[b] $T=60\pm3$	Nb_3F_{15}[d] $T=60\pm10$	Mo_3F_{15}[e] $T=60\pm10$	Ru_3F_{15}[f] $T=80\pm10$	Ta_3F_{15}[b] $T=20\pm2$	Au_3F_{15}[b] $T=205\pm10$	Au_2F_{10}[b] $T=205\pm10$	Sb_3F_{15}[b] "chair", C_{3v} $T=20\pm2$	Sb_3F_{15}[b] "boat", C_s $T=20\pm2$
$M–F_{ax}$	1.810(2)[c]	1.815(4)	1.797(6)	1.818(7)	1.846(5)	1.889(9)	1.889(9)	1.812(2)	1.811(2)
$M–F_t$	1.810(2)	1.815(4)	1.797(6)	1.757(15)	1.823(5)	1.822(8)	1.822(8)	1.812(2)	1.811(2)
$M–F_b$	2.046(4)	2.047(6)	2.007(10)	1.981(5)	2.062(2)	2.030(7)	2.030(7)	2.045(4)	2.044(4)
$\angle F_aMF_a$	162.5(1.4)	165.9(1.5)	160.0(1.5)	181.0(1.0)	173.1(2.1)	193.1(3.2)	181.0(1.1)	160.5(1.2)	161.6(1.7)
$\angle F_tMF_t$	102.9(1.2)	101.1(2.8)	100.5(2.5)	96.0(2.0)	96.4(1.5)	75.3(6.5)	93.3(1.7)	96.7(1.7)	98.2(1.9)
$\angle F_bMF_b$	82.0(1.0)	80.6(1.8)	79.5(1.5)	89.0(1.0)	83.5(0.6)	115.7(1.1)	80.1(0.5)	80.9(1.1)	81.5(1.5)
$\angle MF_bM$	158.0(1.0)	159.4(1.8)	160.5(1.6)	151.0(1.0)	156.5(1.0)	124.3(1.1)	99.9(0.5)	149.7(1.0)	149.7(1.0)
R_f/%	10.2	10.3	13.0	5.4	7.4	4.08	4.08	6.4	6.2

[a]Distances in Å, angles in degrees, temperature (T) in °C. [b]Ref. 170. [c]1 standard deviation (σ). [d]Ref. 174. [e]Ref. 175. Ref. 181.

provement in the agreement between the experimental and theoretical intensities. The radial distribution curves for $(TaF_5)_3$ and $(NbF_5)_3$ are given in Fig. 11 and Fig. 12, respectively.

Antimony pentafluoride. Electron diffraction patterns for antimony pentafluoride were obtained at 20(2) °C. The experimental details are given in Ref. 170. The analysis was performed as described above using the gas-phase vibrational frequencies reported in Ref. 180. The best fit was obtained for trimeric $(SbF_5)_3$ molecules of C_s symmetry (Fig. 11b), whereas the D_{3h} model with a planar six-membered ring with alternating Sb and F atoms gave far poorer agreement.

The molecular parameters for $(SbF_5)_3$ obtained taking triatomic scattering into consideration[123] are listed in Table 3. The dihedral angle made by the planes containing atoms (6, 12, 18) and (1, 6, 18), respectively, is 34.2°. A C_{3v} model provides an equally good fit. The corresponding angle is then 13.2°. The radial distribution curves for $(SbF_5)_3$ are shown in Fig. 12.

Gold pentafluoride. The electron diffraction patterns for gaseous gold pentafluoride were recorded at 210(10) °C. The experimental details and initial data processing are described in Ref. 172. A combined analysis of the electron diffraction and spectroscopic data was carried out using the frequencies reported in Refs. 140 and 141 for AuF_5 crystals. For this reason, only the l and D values for three (Au–F)-type distances were used in the refinement of the force field (Table 3).

Even at the preliminary stage, the radial distribution curve for AuF_5 (Fig. 13) showed the presence of $(AuF_5)_2$ dimers as the major gas-phase component. Applying the minimization procedure to scattering intensities[178,179] led to a D_{2h} model with three types of atomic spacings, viz. the axial, terminal and bridge spacings (Fig. 13). To obtain satisfactory agreement with the assumption of the presence of only Au_2F_{10} molecules of D_{2h} symmetry, the amplitudes for the non-bonded (Au ··· Au) and (Au ··· F) distances were refined. The quantities thus obtained were too large compared with those calculated using the harmonic approximation and the model force field for Au_2F_{10} consistent with the spectroscopic data.[140,141] Attempts to increase the amplitudes by decreasing the torsional force constant responsible for $Au_1F_9Au_7F_{12}$ ring deformations did not result in any significant improvement. At the same time the experimental and theoretical radial distribution curves (Fig. 14) were markedly different in the region from 3.0 to 3.7 Å, a 3.6 Å peak of the experimental curve (Fig. 13) being absent in the theoretical curve. As the (Au ··· Au) distance in the dimer is somewhat smaller, the 3.6 Å peak may correspond to the (Au ··· Au) distance in a trimer, $(AuF_5)_3$. Further refinements demonstrated that this was the case and that the initial assumption of the equality of the (Au–F) distances in the dimeric and the tri-

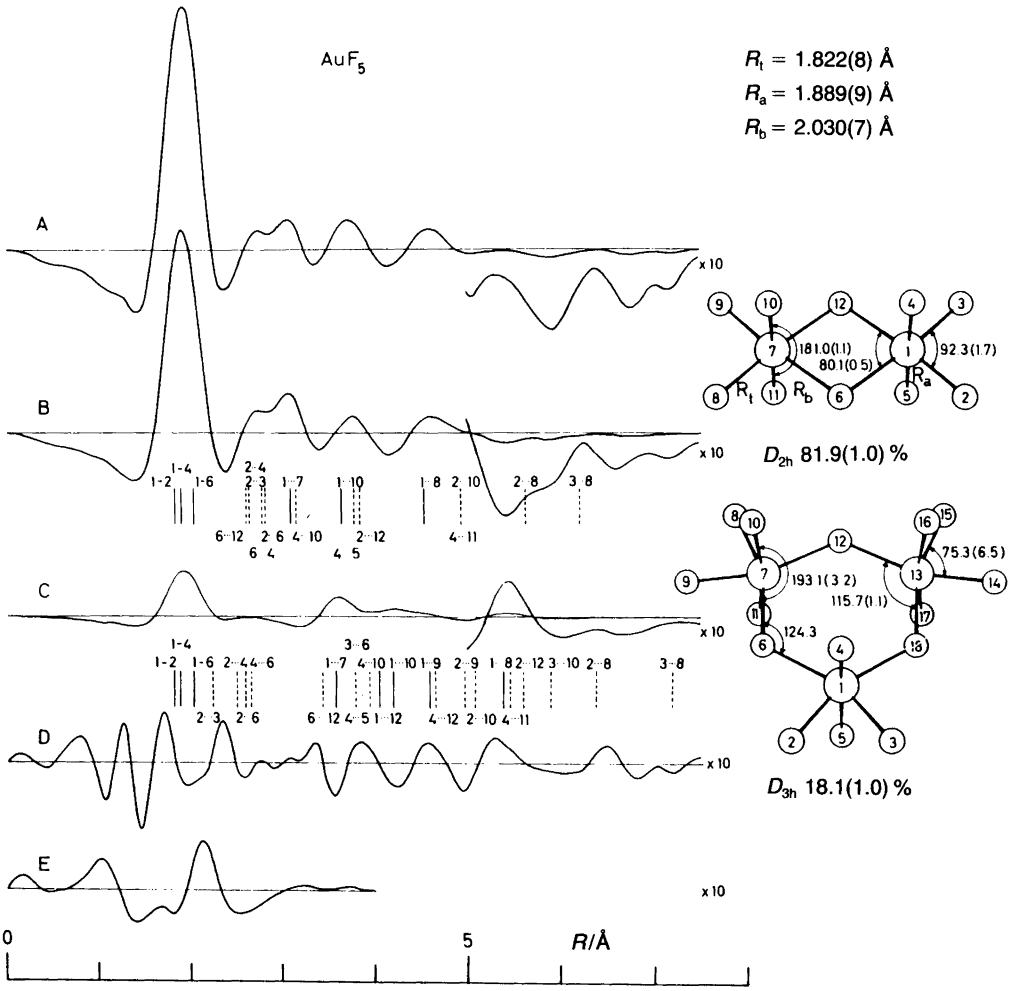

Fig. 13. Radial distribution curve for gold pentafluoride, and molecular models for Au_2F_{10} and Au_3F_{15}.

meric species could not be relaxed. Varying amplitudes for (Au ··· Au) and (Au ··· F) distances had no significant effect on the agreement between the curves, and amplitude variations were only small, which was considered as an indication of consistency between the electron-diffraction and spectroscopic data.

The results are listed in Table 3 and represented in Fig. 13. The best fit is obtained with the assumption of the presence of two gas-phase components, namely $(AuF_5)_2$ molecules of D_{2h} symmetry and $(AuF_5)_3$ ones of D_{3h} symmetry. The analysis was carried out using a non-diagonal weight matrix.[179] Of the correlation coefficients, three exceeded 0.70: $\varrho[\Delta r/r_\alpha(\text{Au–F}_1)] = -0.94$; $\varrho[r_\alpha(\text{Au–F}_6) / \angle_\alpha(\text{F}_b\text{–M–F}_b)_{\text{dimer}}] = 0.91$, and $\varrho[r_\alpha(\text{Au–F}_b) / \angle_\alpha(\text{F}_b\text{–Au–F}_b)_{\text{trimer}}] = 0.73$. At the final refinement stage, triatomic scattering contributions were included[123] which reduced the R_f factor from 4.85 to 4.08 %.

Discussion of the results

As follows from our analysis of electron diffraction data on pentafluoride molecules, the principal information on the degree of their association in the gas phase is provided by the shape of peaks in the region of non-bonded (M ··· M) distances

and the heights of these peaks relative to the peaks corresponding to bonded (M–F) distances. The ratio of the number of (M–F) distances to the number of (M ··· M) ones is equal to 12:1, 18:3 and 24:6 for dimeric, trimeric and tetrameric species, respectively. From this it follows that an incorrect assumption concerning the gas-phase composition should immediately result in a disagreement in the corresponding distances. Besides, tetrameric molecules are expected to contain non-bonded M ··· M distances of two types. The agreement attained for trimeric $(NbF_5)_3$, $(TaF_5)_3$ and $(SbF_5)_3$ species, and a mixture of $(AuF_5)_2$ dimers and $(AuF_5)_3$ trimers is quite satisfactory. It follows from the R_f value (Table 3) that the presence of other molecular forms in substantial amounts can hardly be expected. Distortion of D_{3h} (or D_{2h} for gold pentafluoride) nuclear configurations does not result in an improvement in the agreement between the experimental and theoretical curves for niobium, tantalum and gold pentafluorides. The six-membered rings in $(NbF_5)_3$, $(TaF_5)_3$ and $(AuF_5)_3$ should therefore be planar or nearly planar. These results agree with those of the more recent study of $(NbF_5)_3$[174] and the data on $(MoF_5)_3$[175] and $(RuF_5)_3$[181] obtained using a similar technique of co-refinement of electron diffraction and spectroscopic experiments.

The six-membered ring with alternating Sb and F atoms in $(SbF_5)_3$ deviates significantly from planarity. The Sb ··· Sb distance in this molecule of 3.95 Å is too long to expect that internuclear repulsions would be important.[182] A plausible explanation is that the *d* orbitals on Nb and Ta atoms participate in the formation of delocalized π-electron systems stabilizing the planar ring structures.[183] As antimony 4*d* orbitals are filled, the formation of π molecular orbitals in the antimony derivative is less probable.

The experimental data on $(SbF_5)_3$ fit the "chair" and "boat" conformations (Figs. 11b and 11c) equally well, the R_f values being 6.4 and 6.2 %, respectively. The difference curves for the two models are also similar to each other (Fig. 13). A refinement for a mixture of the two conformers can therefore hardly be expected to improve the fit or provide information about their relative abundances in the gas phase. It seems most reasonable to assume the two conformers to be energetically equivalent and to undergo practically free interconversion. If the entropy of the two forms otherwise differs only insignificantly, the "boat" conformer should constitute 75 % in the gas phase, as the symmetry numbers of the conformers are related as 3:1. The structure parameters of the (–SbF_6–) units in the two forms are quite similar (Table 3).

The data obtained on the composition of vapour over gold pentafluoride agree with those determined by mass-spectrometry at 85–90 °C.[184] According to mass-spectrometric measurements, stable M_2F_{10} dimers also exist in platinum[185] and uranium[186] pentafluorides.

The Au–F_{ax} distances are somewhat larger than the terminal ones, and the average $\langle r_\alpha(\text{Au–F})\rangle$ = 1.856 Å coincides with that found for $Xe_2F_{11}^+$ AuF_6^-.[187]

No significant differences between axial and equatorial bond lengths have been observed for trimeric Nb, Ta and Sb pentafluorides, whereas for $(TaF_5)_3$, $(RuF_5)_3$ and $(AuF_5)_3$, Δr_{ax-t} = 0.023(11) Å, 0.061(15) Å and 0.067(9) Å, respectively (Table 3).

Assuming that Δr_{ax-t} in $(NbF_5)_3$ and $(TaF_5)_3$ actually is small, one is lead to conclude that the terminal bond lengths for $(NbF_5)_3$, $(TaF_5)_3$ and $(SbF_5)_3$ fall within a narrow range of 1.810(2) Å [for $(NbF_5)_3$] to 1.823(5) Å [for $TaF_5)_3$]. These values are close to the values found for $(NbF_5)_3$ and $(TaF_5)_3$[136] in the crystalline state. The same is true for the (M–F_b) distances in $(TaF_5)_3$, $(NbF_5)_3$ and $(SbF_5)_3$.[139,188] The bridge r_α(M–F_b) bond lengths in molybdenum and ruthenium pentafluorides are far shorter than in other molecules studied and than the crystal state parameters of MoF_5[134] and RuF_5.[137]

The r_α(Au ··· Au) distances in $(AuF_5)_2$, 3.107(5) Å, and $(AuF_5)_3$, 3.589(12) Å, are far shorter than the corresponding distances in the other metal pentafluorides (Table 5), which are in the range 3.84 to 4.04 Å. As a consequence, the angle $\angle_\alpha(F_b\text{–Au–}F_b)$ = 115.7(1.1)° in $(AuF_5)_3$ is larger than the corresponding values of 80 to 89° in other metal pentafluorides.

The axial fluorine atoms in Nb, Mo, Sb and Ta pentafluorides are strongly displaced towards the ring axes. With $(RuF_5)_3$, $(AuF_5)_3$ and $(AuF_5)_2$, displacements in the opposite direction are observed. These are especially large for $(AuF_5)_3$. This can be explained on the basis of repulsions between axial fluorine atoms caused by a sub-

stantial shortening of these distances in $(RuF_5)_3$, $(AuF_5)_3$ and $(AuF_5)_2$ relative to $(NbF_5)_3$, $(MoF_5)_3$, $(SbF_5)_3$ and $(TaF_5)_3$.

Acknowledgement. The authors would like to express their hearty thanks to Professor O. Bastiansen, who stimulated and encouraged the Oslo–Moscow cooperation and whose profound influence on electron diffraction studies at Moscow University was highly inspiring.

References

1. Basolo, F. and Pearson, R. G. *Mechanisms of Inorganic Reactions,* 2nd. ed., Wiley, New York 1967, Chap. 2.
2. Ingold, C. K. *Structure and Mechanism in Organic Chemistry,* Cornell University Press, Ithaca, N.Y. 1953, p. 403.
3. Schmutzler, R. *Adv. Fluorine Chem. 5* (1965) 31.
4. Sommer, L. N. *Stereochemistry, Mechanism and Silicon: An Introduction to the Dynamic Stereochemistry and Reaction Mechanisms of Silicon Centers* (McGraw Hill Series in Advanced Chemistry), McGraw Hill, New York 1965, p. 189.
5. Hudson, R. F. *Structure and Mechanisms in Organophosphorus Chemistry,* Academic Press, New York 1965.
6. Pearson, R. G. *Symmetry Rules for Chemical Reactions,* Wiley, New York 1976.
7. Vilkov, L. V. and Naumow, V. A. *Molecular Structures of Phosphororganic Compounds,* Moscow 1986 (in Russian).
8. Westheimer, F. H. *Acc. Chem. Res. 1* (1968) 70.
9. Mislov, K. *Acc. Chem. Res. 3* (1970) 321.
10. Muetterties, E. L. and Schann, R. A. *Quart. Rev. Chem. Soc. 20* (1966) 245.
11. Muetterties, E. L. *J. Am. Chem. Soc. 91* (1969) 1636.
12. Boldyrev, A. I. and Charkin, O. P. *Zh. Strukt. Khim. 25* (1984) 102.
13. Pershin, V. L. and Boldyrev, A. I. *J. Mol. Struct. (Theochem) 150* (1987) 171.
14. Crotov, S. S., Ischenko, A. A. and Ivashkevich, L. S. *Int. J. Quantum Chem. 16* (1979) 973.
15. Berry, R. S. *J. Chem. Phys. 32* (1960) 933.
16. Gillespie, R. J. *Molecular Geometry,* Van Nostrand Reinhold, London 1972.
17. Bartell, L. S. and Plato, V. *J. Am. Chem. Soc. 95* (1973) 3097.
18. Hargittai, I. *Inorg. Chem. 21* (1982) 4334.
19. Bartell, L. S. *Croat. Chem. Acta 57* (1984) 927.
20. Kepert, D. L. *Inorganic Stereochemistry,* Springer-Verlag, Berlin, Heidelberg, New York 1982.
21. Downs, J. J. and Johnson, R. E. *J. Chem. Phys. 22* (1954) 143.
22. Downs, J. J. and Johnson, R. E. *J. Am. Chem. Soc. 77* (1955) 2098.
23. Muetterties, E. L. *Acc. Chem. Res. 3* (1970) 266.
24. Gutowsky, H. S. and Hoffman, C. J. *Phys. Rev. 80* (1950) 110.
25. Gutowsky, H. S., McCall, D. W. and Slichter, C. P. *J. Chem. Phys. 21* (1953) 279.
26. Bramley, R., Figgis, B. N. and Nyholm, R. S. *Trans. Faraday Soc. 58* (1962) 1893.
27. Mucher, J. I. *J. Chem. Educ. 51* (1974) 94.
28. Brockway, L. O. and Beach, J. J. *J. Am. Chem. Soc. 60* (1938) 1836.
29. Roualt, M. *Ann. Phys. (Paris) 14* (1940) 78.
30. Hansen, K. W. and Bartell, L. S. *Inorg. Chem. 4* (1965) 1775.
31. Spiridonov, V. P., Ischenko, A. A. and Ivashkevich, L. S. *J. Mol. Struct. 72* (1981) 153.
32. Adams, W. J. and Bartell, L. S. *J. Mol. Struct. 8* (1971) 23.
33. Muetterties, E. L. *Inorg. Chem. 4* (1965) 769.
34. Muetterties, E. L. and Knoth, W. H. In: Dekker, H., Ed., *Polyhedral Boranes,* New York 1968, p. 197.
35. Muetterties, E. L. *Rec. Chem. Progr. 31* (1971) 51.
36. Sergeev, N. M. *Russ. Chem. Rev. 42* (1973) 769.
37. Sergeev, N. M. In: Emsley, J. W., Feeney, J. and Sutcliffe, L. H., Eds., *Progress in NMR Spectroscopy,* Pergamon Press, Oxford 1973, Vol. 9, Part 2, p. 71.
38. Bastiansen, O., Seip, H. M. and Boggs, J. E. In: Dunitz, J. L. and Ibers, J. A., Eds., *Perspectives in Structural Chemistry,* Wiley, New York 1971, Vol. 4, p. 60.
39. Bastiansen, O., Kveseth, K. and Møllendal, H. *Topics Curr. Chem. 81* (1979) 99.
40. Natanson, G. A. *Mol. Phys. 46* (1982) 481.
41. Kuchitsu, K. In: Allen, G., Ed., *MTP International Review of Science, Physical Chemistry Ser. 1,* Butterworths, London 1972, Vol. 2, Chap. 6.
42. Karle, J. In: Nachod, F. C. and Zuckerman, J. J., Eds., *Determination of Organic Structures,* Academic Press, New York 1973.
43. Cotton, F. A. *Acc. Chem. Res. 1* (1968) 257.
44. Papousek, D. and Aliev, M. R. *Molecular Vibrational, Rotational Spectra,* Academia Prague 1982.
45. Spiridonov, V. P., Ischenko, A. A. and Zasorin, E. Z. *Russ. Chem. Rev. 47* (1978) 54.
46. Charkin, O. P. and Boldyrev, A. I. *Potential Surfaces and Structural Nonrigidity of Inorganic Molecules. Ser. Inorg. Chem.* VINITI, Moscow 1980, Vol. 8, p. 1560 (in Russian).
47. Bersuker, I. B. *The Structure and Properties of Coordination Compounds,* Khimiya, Leningrad 1986 (in Russian).
48. Vilkov, L. V. and Pentin, Yu. A. *Physical Methods in Chemistry,* High School, Moscow 1987 (in Russian).

49. Wooley, R. G. *Adv. Phys. 25* (1976) 27.
50. Rambidi, N. G. *Strukt. Khim. 23* (1986) 113.
51. Ischenko, A. A., Strand, T. G., Demidov, A. V. and Spiridonov, V. P. *J. Mol. Struct. 43* (1978) 227.
52. Townes, C. H. and Schawlow, A. L. *Microwave Spectroscopy,* McGraw Hill, New York 1977.
53. Claverie, P. and Jona-Lasinio, G. *Phys. Rev. A 33* (1986) 2245.
54. Boldyrev, A. I. and Onischuk, A. V. *Zh. Fiz. Khim. In press.*
55. Dennison, D. M. and Uhlenbeck, G. E. *Phys. Rev. 41* (1932) 313.
56. Benedict, W. S. and Plyler, E. L. *Can. J. Phys. 35* (1957) 1235.
57. Jona-Lasinio, G., Martinelli, F. and Scoppolle, E. *Phys. Rev. 77* (1981) 223.
58. Jona-Lasinio, G., Martinelli, F. and Scoppolle, E. *Commun. Mat. Phys. 80* (1981) 223.
59. Graffi, S., Grecchi, V. and Joan-Lasionio, G. *J. Phys. A: Math. Gen. 17* (1985) 2935.
60. Helffer, B. and Sjöstrand, J. *Ann. Institute H. Poincaré (Phys. Theor.) 42* (1985) 127.
61. Simon, B. *J. Funct. Anal. 63* (1985) 123.
62. Bunker, P. R. *Molecular Symmetry and Molecular Structures,* Academic Press, New York 1979.
63. Lauterbur, P. C. and Ramirez, F. *J. Am. Chem. Soc. 90* (1968) 6722.
64. Strich, A. and Veillard, A. *J. Am. Chem. Soc. 95* (1973) 5574.
65. Demuynck, J., Strich, A. and Veillard, A. *Nouv. J. Chim. 1* (1977) 217.
66. Marsden, C. J. *J. Chem. Soc., Chem. Commun.* (1984) 401.
67. Almlöf, J. and Ischenko, A. A. *Abstracts of the VIII All-Union Symposium on Physical and Mathematical Methods in Coordination Chemistry,* Kishimev 1983, p. 229 (in Russian).
68. Ugi, I., Marguarding, D., Klusacek, H., Gillespie, P. and Ramires, F. *Acc. Chem. Res. 4* (1971) 288.
69. Meakin, P., Muetterties, E. L. and Jesson, J. P. *J. Am. Chem. Soc. 94* (1972) 5271.
70. Muetterties, E. L. and Hirsekorn, F. J. *J. Am. Chem. Soc. 95* (1973) 5419.
71. Miller, J. S. and Caulton, K. G. *Inorg. Chem. 14* (1975) 2296.
72. Meakin, P., Muetterties, E. L. and Jesson, J. P. *J. Am. Chem. Soc. 94* (1972) 5271.
73. Muetterties, E. L. In: Tobe, M. L., Ed., *MTP International Review of Science, Inorganic Chemistry, Ser. 1,* Butterworths, London 1972, Vol. 9, Chap. 2.
74. Jesson, J. P. and Meakin, P. *J. Am. Chem. Soc. 96* (1974) 5760.
75. Debye, P. *J. Chem. Phys. 9* (1941) 55.
76. Cyvin, S. J. *Molecular Vibrations and Mean Square Amplitudes,* Universitetsforlaget, Oslo 1968.
77. Morino, Y. and Hirota, E. *J. Chem. Phys. 28* (1958) 185.
78. ter Brake, J. H. M. *On Large-Amplitude Motion and the Background in Electron Diffraction.* Ph. D. thesis, University of Leiden, Leiden 1986.
79. Beattie, I. R., Gilson, T. R. and Ozin, G. A. *J. Chem. Soc.* (1968) 1092.
80. Beattie, I. R. and Ozin, G. A. *J. Chem. Soc. A* (1969) 1691.
81. Zavalishin, N. *Cand. Diss.,* University of Moscow, Moscow 1975.
82. Witt, J. D., Carreira, L. A. and Durig, J. R. *J. Mol. Struct. 18* (1973) 157.
83. Bernstein, L. S., Kim, J. J., Pitzer, K. S., Abramowits, S. and Levin, I. W. *J. Chem. Phys. 62* (1975) 3671.
84. Bernstein, L. S., Abramowits, S. and Levin, I. W. *J. Chem. Phys. 64* (1976) 3228.
85. Abramowits, S. *Spectrochim. Acta, Part A 42* (1986) 342.
86. Demidov, A. V., Ivanov, A. A., Ivashkevich, L. S., Ischenko, A. A., Spiridonov, V. P., Almlöf, J. and Strand, T. G. *Chem. Phys. Lett. 64* (1979) 528.
87. Spiridonov, V. P., Ischenko, A. A. and Ivashkevich, L. S. *Abstracts of the Eighth Austin Symposium on Molecular Structure,* Austin, Texas 1980, p. 103.
88. Ischenko, A. A., Spiridonov, V. P., Tarasov, Yu. I. and Stuchebrukhov, A. A. *J. Mol. Struct. 172* (1988) 275.
89. Ivashkevich, L. S., Ischenko, A. A., Spiridonov, V. P. and Romanov, G. V. *J. Mol. Struct. 51* (1979) 217.
90. Ogurtsov, I. Ya., Kazantseva, L. A. and Ischenko, A. A. *J. Mol. Struct. 41* (1977) 243.
91. Sellers, H. L. and Schäfer, L. *J. Mol. Struct. 51* (1979) 117.
92. Kuester, J. L. and Mize, J. H. *Optimization Technique with Fortran,* McGraw-Hill, New York 1973, p. 309.
93. Hoffmann, R., Howell, J. M. and Muetterties, E. L. *J. Am. Chem. Soc. 94* (1972) 3047.
94. Gillespie, P., Hoffmann, P., Klusacek, H., Marguarding, D., Prohl, S., Ramirez, F., Tsolis, E. A. and Ugi, I. *Angew. Chem. Int. Ed. Engl. 10* (1971) 687.
95. Berry, R. S., Tamres, M., Ballhausen, C. J. and Johansen, H. *Acta Chem. Scand. 22* (1968) 231.
96. Van der Voorn, P. C. and Drago, R. S. *J. Am. Chem. Soc. 88* (1966) 3255.
97. Brown, R. D. and Peel, J. B. *Aust. J. Chem. 21* (1968) 2605; *Ibid.* 2617.

98. Russegger, P. and Brickman, J. *Chem. Phys. Lett. 30* (1975) 276.
99. Strich, A. *Ph. D. Thesis,* University of Strasbourg, Strasbourg 1978.
100. Karimura, H., Yamamoto, S., Egawa, T. and Kuchitsu, K. *J. Mol. Struct. 140* (1986) 79.
101. Kuchitsu, K. and Cyvin, S. J. In: Cyvin, S. J., Ed., *Molecular Structure and Vibrations,* Elsevier, Amsterdam 1972, Chap. 12.
102. Talami, M. and Kuze, H. *J. Chem. Phys. 80* (1984) 2314.
103. Yamamoto, S., Takami, N. and Kuchitsu, K. *J. Chem. Phys. 82* (1985) 3879.
104. Ivashkevich, L. S., Ischenko, A. A., Spiridonov, V. P., Strand, T. G., Ivanov, A. A. and Nikolaev, A. V. *Zh. Strukt. Khim. 23* (1982) 144.
105. Roualt, M. *Ann. Phys. (Paris) 14* (1940) 78.
106. Ohlberg, S. M. *J. Am. Chem. Soc. 81* ((1959) 811.
107. Holmes, R. R. and Deiters, R. M. *Inorg. Chem. 7* (1968) 2229.
108. Holmes, R. R., Deiters, R. M. and Golen, J. A. *Inorg. Chem. 8* (1969) 2612.
109. Holmes, R. R. *Acc. Chem. Res. 5* (1972) 296.
110. Selig, H., Holloway, J. H., Tyson, J. and Claasen, H. H. *J. Chem. Phys. 53* (1970) 2559.
111. Skinner, H. A. and Sutton, L. E. *Trans. Faraday Soc. 36* (1940) 668.
112. Spiridonov, V. P. and Romanov, G. V. *Vestn. Mosk. Univ. Khim. 21* (1966) 109.
113. Spiridonov, V. P. and Romanov, G. V. *Vestn. Mosk. Univ. Khim. 23* (1968) 10.
114. Clippard, F. B. and Bartell, L. S. *Inorg. Chem. 9* (1970) 805.
115. Pyykkö, P. In: Löwdin, P.-O., Ed., *Adv. Quantum Chem. 9* (1979).
116. Zalkin, A. and Sands, D. *Acta Crystallogr. 11* (1958) 615.
117. Zalkin, A., Sands, D. and Elson, R. *Acta Crystallogr. 12* (1959) 21.
118. Preiss, H. *Z. Anorg. Allg. Chem. 389* (1972) 280.
119. Bennett, L. S., Margrave, J. L. and Franklin, J. L. *J. Inorg. Nucl. Chem. 37* (1975) 937.
120. Berdonosov, S. S., Lapitskii, P. V. and Bakov, E. K. *Zh. Neorg. Khim. 10* (1965) 322.
121. Spiridonov, V. P. and Romanov, G. V. *Vestn. Mosk. Univ. Khim. 6* (1966) 109.
122. Bartell, L. S. *J. Chem. Phys. 63* (1975) 3750.
123. Miller, R. B. and Bartell, L. S. *J. Chem. Phys. 72* (1980) 800.
124. Laane, J. *Appl. Spectrosc. 24* (1970) 73.
125. Krasnov, K. S. *Molecular Constants of Inorganic Compounds,* Khimiya, Leningrad 1979 (in Russian).
126. Suzuki, I. *Bull. Chem. Soc. Jpn. 44* (1971) 3277.
127. Gribov, L. A. *Opt. Spectrosk. 31* (1971) 842.
128. Vol'kenshtein, M. A., Gribov, L. A., El'jashevich, M. A. and Stepanov, B. I. *Molecular Vibrations,* Moscow 1972, p. 699 (in Russian).
129. Miller, B. R. and Fink, M. J. *J. Chem. Phys. 75* (1981) 5326.
130. Konaka, S., Sasaki, Y. and Kimura, M. *J. Mol. Struct. 88* (1982) 387.
131. Bonham, R. A. and Schäfer, L. In: *International Tables for X-Ray Crystallography,* The Kynoch Press, Birmingham 1974, Vol. IV.
132. Canterford, J. H. and Colton, R. *Halides of the Second and Third Row Transition Metals,* Wiley, New York 1968, p. 19.
133. Fairbrother, F. *The Chemistry of Niobium and Tantalum,* Elsevier, Amsterdam 1967.
134. Opalowskii, A. A., Tichinskaya, I. I., Kuznetsova, Z. M. and Samoilov, P. P. *Halogenides of Molybdenum,* Novosibirsk 1972, p. 259 (in Russian).
135. Wykoff, R. W. G. *Crystal Structures,* 2nd. ed., Wiley Interscience, New York 1964, Vol. 2, p. 174.
136. Edwards, A. J. *J. Chem. Soc. 10* (1964) 3714.
137. Holloway, J. H., Peacock, R. D. and Small, R. W. H. *J. Chem. Soc.* (1964) 644.
138. Edwards, A. J., Jones, G. R. and Steventon, B. R. *J. Chem. Soc., Chem. Commun.* (1967) 462.
139. Edwards, A. J. and Taylor, P. *J. Chem. Soc., Chem. Commun.* (1971) 1376.
140. Sokolov, V. B. and Prusakov, V. N. *Abstracts of the IV All-Union Symposium on Chemistry of Inorganic Fluorides,* Dushanbe 1975, p. 193 (in Russian).
141. Sololov, V. B., Prusakov, V. N., Rizkov, A. V., Drobishevski, Y. V. and Khoroshev, S. S. *Dokl. Akad. Nauk SSSR 229* (1976) 884.
142. Kleinschmidt, P. D. and Hildenbrand, D. L. *J. Chem. Phys. 71* (1979) 196.
143. Beattie, I. R., Livingston, K. M. S., Ozin, G. A. and Reinolds, D. R. *J. Chem. Soc. A* (1969) 958.
144. Quelette, T. J., Ratcliffe, C. T. and Sharp, D. W. A. *J. Chem. Soc. A* (1969) 2351.
145. Seilig, H., Reis, A. and Casner, E. L. *J. Inorg. Nucl. Chem. 30* (1968) 2087.
146. Hoffman, C. J., Holder, B. E. and Jally, W. L. *J. Phys. Chem. 62* (1958) 364.
147. Muetterties, E. L. and Philips, W. D. *J. Am. Chem. Soc. 82* (1959) 1084.
148. Fairbrother, F., Grundy, K. H. and Thompson, A. *J. Chem. Soc.* (1965) 765.
149. Wolf. A. A. and Greenwood, W. N. *J. Chem. Soc.* (1950) 2200.
150. Romanov, G. V. and Spiridonov, V. P. *Izv. Sib. Otd. Akad. Nauk SSSR, Ser. Khim. Nauk, 1* (1968) 126.
151. Romanov, G. V. and Spiridonov, V. P. *Vestn. Mosk. Univ. Khim. 23* (1968) 7 (in Russian).
152. Alexander, L. E., Beattie, I. R. and Jones, R. J. *J. Chem. Soc., Dalton Trans.* (1972) 210.

153. Petrova, V. N., Girichev, G. V., Petrov, V. M. and Goncharuk, V. K. *Zh. Strukt. Khim. 26* (1985) 56.
154. Petrova, V. N., Girichev, G. V. and Petrov, V. M. *Abstracts of the VII All-Union Symposium on Chemistry of Inorganic Fluorides,* Dushanbe 1984, p. 264 (in Russian).
155. Acguista, N. and Abramowitz, S. *J. Chem. Phys. 56* (1972) 5221.
156. Vasile, M. J., Jones, G. R. and Falconer, W. E. *J. Chem. Soc., Chem. Commun.* (1971) 1355.
157. Gotkis, I. S. *Cand. Dissertation,* Moscow University, Moscow 1975 (in Russian).
158. Gotkis, I. S., Gusarov, A. V. and Gorokhov, L. N. *Zh. Neorg. Khim. 20* (1975) 1250.
159. Fawcett, J., Hewitt, A. J., Holloway, J. H. and Stephen, M. A. *J. Chem. Soc., Dalton Trans.* (1976) 2422.
160. Falconer, W. E., Jones, G. R., Sander, W. A. and Vasile, M. J. *J. Fluorine Chem. 4* (1974) 213.
161. Tikhonov, A. N. and Arsenin, V. Ya. *Methods of Solution of Ill-posed Problems,* Nauka, Moscow 1979, p. 285 (in Russian).
162. Tikhonov, A. N., Ed., *Mathematical Modelling Methods, Automatization of Experiments, Observations Treatment and its Applications,* Moscow University, Moscow 1986, p. 217 (in Russian).
163. Tikhonov, A. N., Goncharskii, A. V., Stepanov, V. V. and Yagola, A. G. *Regularization Algorithms and a priori Information,* Nauka, Moscow 1983, p. 197 (in Russian).
164. Herzberg, G. *Vibrational and Rotational Spectra of Polyatomic Molecules,* Wiley, New York 1949, p. 648.
165. Kochikov, I. V., Kuramshina, G. M., Pentin, Yu. A. and Yagola, A. G. *Dokl. Akad. Nauk. SSSR 261* (1981) 1104.
166. Kochikov, I. V., Kuramshina, G. M. and Pentin, Yu. A. *Zh. Fiz. Khim. 61* (1987) 865.
167. Bastiansen, O. and Trætteberg, M. *Acta Crystallogr. 13* (1960) 1108.
168. Morino, Y. *Acta Crystallogr. 13* (1960) 1107.
169. Cyvin, S. J., In: Cyvin, S. J., Ed., *Molecular Structure and Vibrations,* Elsevier, Amsterdam 1975, p. 95.
170. Brunvoll, J., Ischenko, A. A., Miakshin, I. N., Romanov, G. V., Sokolov, V. B., Spiridonov, V. P. and Strand, T. G. *Acta Chem. Scand., Ser. A 34* (1980) 733.
171. Brunvoll, J., Ischenko, A. A., Miakshin, I. N., Romanov, G. V., Sokolov, V. B., Spiridonov, V. P. and Strand, T. G. *Acta Chem. Scand., Ser. A 33* (1979) 775.
172. Brunvoll, J., Ischenko, A. A., Ivanov, A. A., Romanov, G. V., Sokolov, V. B., Spiridonov, V. P. and Strand, T. G. *Acta Chem. Scand., Ser. A 36* (1982) 705.
173. Brunvoll, J., Ischenko, A. A., Spiridonov, V. P. and Strand, T. G. *Acta Chem. Scand., Ser. A 38* (1984) 115.
174. Girichev, G. V., Petrova, V. N., Petrov, V. M. and Krasnov, K. S. *Koord. Khim. 9* (1983) 799.
175. Girichev, G. V., Petrova, V. N., Petrov, V. M. and Krasnov, K. S. *Zh. Strukt. Khim. 24* (1983) 54.
176. Girichev, G. V., Petrova, V. N., Rakov, E. G., Utkin, A. N., Dudin, A. S. and Djanavjan, A. V. *Abstracts of the VII All-Union Symposium on Chemistry of Inorganic Fluorides,* Dushanbe 1984, p. 107 (in Russian).
177. Ivanov, A. A., Spiridonov, V. P., Demidov, A. V. and Zasorin, E. Z. *Prib Tekh. Eksp. 2* (1974) 270.
178. Andersen, B., Seip, H. M., Strand, T. G. and Stølevik, R. *Acta Chem. Scand. 23* (1969) 3224.
179. Seip, H. M., Strand, T. G. and Stölevik, R. *Chem. Phys. Lett. 3* (1969) 617.
180. Alexander, L. E. and Beattie, I. R. *J. Chem. Phys. 56* (1972) 5829.
181. Petrova, V. I. *Cand. Dissertation,* Ivano 1985 (in Russian).
182. Glidewell, C. *Inorg. Chim. Acta. 36* (1979) 135.
183. Mitchell, K. A. R. *Chem. Rev. 69* (1969) 157.
184. Vasile, M. J., Richardson, T. J., Steavie, F. A. and Falconer, W. E. *J. Chem. Soc., Dalton Trans.* (1976) 351.
185. Kuznetsov, S. V., Korobov, M. V., Savinova, L. I. and Sidorov, L. N. *Abstracts of the VIII All-Union Symposium on Chemistry of Inorganic Fluorides,* Tashkent 1987, p. 210 (in Russian).
186. Bondarenko, A. A., Korobov, M. V., Sidorov, L. N. and Karasev, N. M. *Zh. Fiz. Khim. 61* (1987) 2583.
187. Learly, K., Zalkin, A. and Bartlett, N. *Inorg. Chem. 13* (1974) 755.
188. Polinova, T. N. and Porai-Koshits, M. A. *Zh. Strukt. Khim. 7* (1966) 642.

Received January 29, 1988.